

AD-A036 976

DAVID W TAYLOR NAVAL SHIP RESEARCH AND DEVELOPMENT CE--ETC F/G 13/10
FEASIBILITY OF THE USE OF WATERBORNE PROPULSION FOR LARGE AIR C--ETC(U)
FEB 77 G KARAFIATH, T CSAKY

UNCLASSIFIED

SPD-746-01

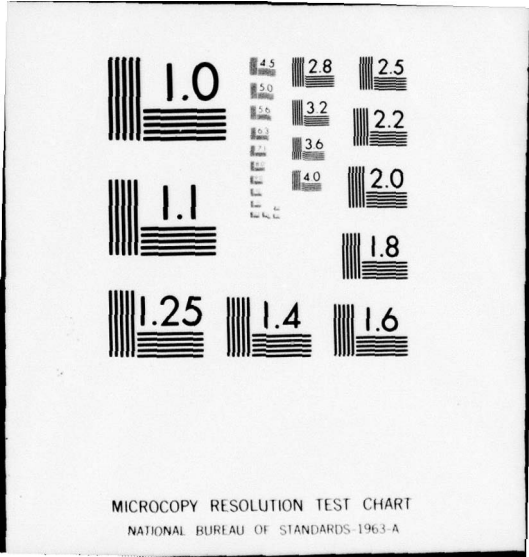
NL

1 of 1
ADA036976



END

DATE
FILMED
4-77



SPD-746-01

FEASIBILITY OF THE USE OF WATERBORNE PROPULSION FOR LARGE AIR CUSHION VEHICLES

ADA 036976

12 B.S.

DAVID W. TAYLOR NAVAL SHIP RESEARCH AND DEVELOPMENT CENTER



Bethesda, Md. 20084

FEASIBILITY OF THE USE OF WATERBORNE
PROPULSION FOR LARGE AIR CUSHION VEHICLES

BY

G. Karafiath and T. Csaky

APPROVED FOR PUBLIC RELEASE: DISTRIBUTION UNLIMITED

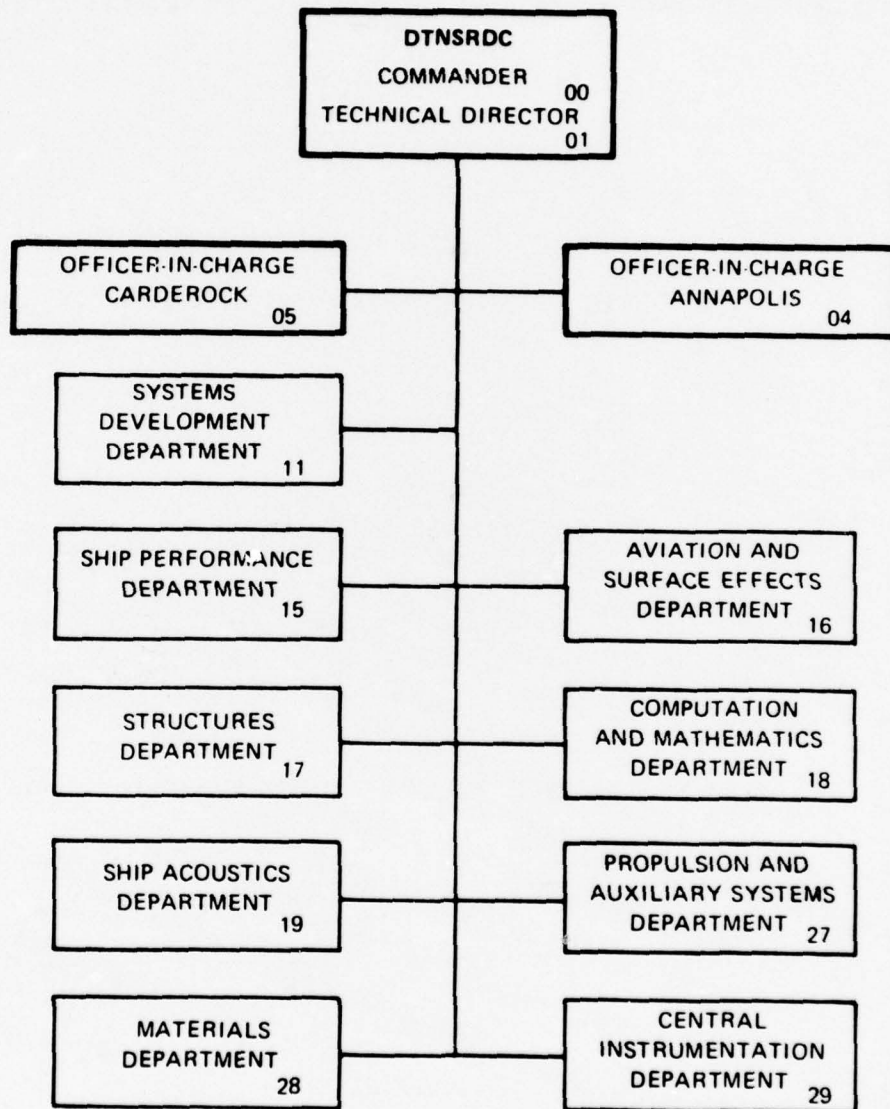
SHIP PERFORMANCE DEPARTMENT
DEPARTMENTAL REPORT

DDC
RECEIVED
MAR 17 1977
C

February 1977

SPD-746-01

MAJOR DTNSRDC ORGANIZATIONAL COMPONENTS



Karafiath
227-1638

TCD #16 Project: Per telecon
w/Karafiath/227-1638/ Proj. 40
NSRDC
should be SSH15 (in agreement
w/ Dept Navy RDT/E Mgt Cd-1495)

[Signature]
22 Mar 77

REPORT DOCUMENTATION PAGE		READ INSTRUCTIONS BEFORE COMPLETING FORM
1. REPORT NUMBER SPD-746-01	2. GOVT ACCESSION NO.	3. RECIPIENT'S CATALOG NUMBER
4. TITLE (and Subtitle) FEASIBILITY OF THE USE OF WATERBORNE PROPULSION FOR LARGE AIR CUSHION VEHICLES		5. TYPE OF REPORT & PERIOD COVERED
7. AUTHOR(s) G. Karafiath and T. Csaky		6. PERFORMING ORG. REPORT NUMBER
9. PERFORMING ORGANIZATION NAME AND ADDRESS David W. Taylor Naval Ship R&D Center Bethesda, Maryland 20084		8. CONTRACT OR GRANT NUMBER(s)
11. CONTROLLING OFFICE NAME AND ADDRESS		10. PROGRAM ELEMENT, PROJECT, TASK AREA & WORK UNIT NUMBERS Task No. SSH15002, Job Order No. 1-1100-700-34 PE 63534N
14. MONITORING AGENCY NAME & ADDRESS (if different from Controlling Office) Naval Sea Systems Command Washington, D.C. 20350		12. REPORT DATE February 1977
16. DISTRIBUTION STATEMENT (of this Report) APPROVED FOR PUBLIC RELEASE: DISTRIBUTION UNLIMITED (16) SSH 15 (12) SSH 15 002		13. NUMBER OF PAGES 11
17. DISTRIBUTION STATEMENT (of the abstract entered in Block 20, if different from Report)		15. SECURITY CLASS. (of this report) UNCLASSIFIED
18. SUPPLEMENTARY NOTES		15a. DECLASSIFICATION/DOWNGRADING SCHEDULE
19. KEY WORDS (Continue on reverse side if necessary and identify by block number) Waterborne Propulsion Air Cushion Vehicles Preliminary Gear Design Strut Pod Performance		
20. ABSTRACT (Continue on reverse side if necessary and identify by block number) Propulsive performance predictions are made for large (1,000, 2,000 and 3,000 ton) Air Cushion Vehicles (ACV) with design speeds of 60, 80 and 100 knots. Several gear train arrangements are investigated and a Z drive with dual downshafts and speed reduction in the pod is selected. Minimum required gear envelopes are used to estimate strut pod sizes. The drag of the resultant bas-vented strut pod system is estimated. The performance of a supercavitating propeller is calculated at hump and design speed. Based on hump and design		

D D C
RECEIVED
MAR 17 1977
REGISTERED
C

next page

389694

13

20. (Cont.)

cont → speed performance, certain craft configurations are selected.



ACCESSION BY	
WTIS	White Section <input checked="" type="checkbox"/>
DDC	Buff Section <input type="checkbox"/>
UNAL	<input type="checkbox"/>
JUSTIFICATION	
BY	
DISTRIBUTION/AVAILABILITY CODES	
Dist.	AVAIL. and/or SPECIAL
A	

UNCLASSIFIED

TABLE OF CONTENTS

	Page
ABSTRACT.....	1
INTRODUCTION.....	1
DESCRIPTION OF LARGE CONCEPTUAL AIR CUSHION VEHICLES.....	2
SELECTION OF PROPULSION TRAIN ARRANGEMENTS.....	3
DETERMINATION OF MINIMUM GEARBOX ENVELOPES.....	7
DETERMINATION OF MINIMUM STRUT THICKNESS AND POD DIAMETER.....	26
PROPELLER SELECTION AND PERFORMANCE.....	27
HYDRODYNAMIC STRUT-POD DESIGN AND PERFORMANCE.....	29
PERFORMANCE ESTIMATES FOR POINT DESIGNS.....	30
THE POWERING FEASIBILITY OF POINT DESIGNS.....	40
2000 TON 80 KNOT DESIGN ARRANGEMENTS AND CHARACTERISTICS.....	42
CONCLUSIONS.....	43
RECOMMENDATIONS.....	46
REFERENCES.....	48

LIST OF FIGURES

	Page
Figure 1 - Single Mesh Bevel Gear - Reduction at Engine.....	49
Figure 2 - Dual Mesh Bevel Gear - Reduction at Engine.....	50
Figure 3 - Single Mesh Bevel Gear System - Reduction in Pod.....	51
Figure 4 - Dual Mesh Bevel Gear System - Reduction in Pod....	52
Figure 5 - Concentric Counterrotating Shafts.....	53
Figure 6 - Schematic of the Lower Bevel Gearbox.....	54
Figure 7 - Estimated Envelope of the Lower Bevel Gearbox.....	55
Figure 8 - Loads on Planet Gear Shaft.....	56
Figure 9 - Schematic of Planetary Gearbox with Stationary Ring Gear.....	57
Figure 10 - Schematic of Planetary-Star Reduction Gearbox....	58
Figure 11 - Schematic of Multi Branched Concentric Double Reduction Gearbox.....	59
Figure 12 - Minimum Shaft Size for Required Horsepower per Shaft and Required RPM.....	60
Figure 13 - Gear Pitch Diameters as a Function of Horsepower/Mesh and Gear RPM.....	61
Figure 14 - Propeller Open Water Performance Characteristics at Hump.....	62
Figure 15 - Propeller Open Water Performance Characteristics at 60 Knots.....	63
Figure 16 - Propeller Open Water Performance Characteristics at 80 Knots.....	64
Figure 17 - Propeller Open Water Performance Characteristics at 100 Knots.....	65

Figure 18 - Predicted Strut Drag.....	66
Figure 19 - Predicted Pod Drag.....	67
Figure 20 - Assumed Off-Design Available Engine Power.....	68
Figure 21 - Sample Drag Curve for 2000 Ton Designs.....	69
Figure 22 - Propeller Operating Conditions for a 2000 Ton, 80 Knot Design.....	70
Figure 23 - Cross Section of 2000 Ton Design with Strut Pivoting at Box Structure Bottom.....	71
Figure 24 - Cross Section of 2000 Ton Design with Strut Pivoting at Nacelle.....	72
Figure 25 - 3-Dimensional View of Strut-Pod and Nacelle.....	73
Figure 26 - 80 Knot 2000 Ton ACV with 3 Engines and 3 Strut Pod Propeller Units.....	74

LIST OF TABLES

	Page
Table 1 - Torque and Bevel Gear Diameters for the Arrange- ments of Figures 1 and 2.....	4
Table 2 - Characteristic Data on Bevel Gears at 4000 RPM.....	6
Table 3 - Reduction Ratios for Assumed Propeller Speeds.....	9
Table 4 - Estimated Envelope of Gearboxes.....	23
Table 5 - Capacities of Spiral Bevel Gears.....	24
Table 6 - Propeller Geometry.....	28
Table 7 - Strut Pod Geometry.....	31
Table 8 - Predicted Performance of 1000 Ton Concepts.....	34
Table 9 - Predicted Performance of 2000 Ton Concepts.....	35
Table 10 - Predicted Performance of 3000 Ton Concepts.....	36
Table 11 - Strut-Pod Added Drag Ratios.....	39
Table 12 - 2000 Ton 80 Knot ACV Characteristics and Dimensions.....	44

ABSTRACT

Propulsive performance predictions are made for large (1,000, 2,000 and 3,000 ton) Air Cushion Vehicles (ACV) with design speeds of 60, 80 and 100 knots. Several gear train arrangements are investigated and a Z drive with dual downshafts and speed reduction in the pod is selected. Minimum required gear envelopes are used to estimate strut-pod sizes. The drag of the resultant base vented strut-pod system is estimated. The performance of a supercavitating propeller is calculated at hump and design speed. Based on hump and design speed performance, certain craft configurations are selected.

ADMINISTRATIVE INFORMATION

This report was prepared under the sponsorship of the Advanced Naval Vehicles Concepts Evaluation (ANVCE) Project. The work was done jointly by DTNSRDC Codes 1532 and 2721 under Task No. SSM 15002, Job Order No. 1-1100-700-34. Transmission related aspects of the work were performed by T. Csaky of Code 2721, and the hydrodynamic performance aspects of the work were done by G. Karafiath of Code 1532.

INTRODUCTION

The purpose of this report is to examine the feasibility of using water propellers with large Air Cushion Vehicles. Conceptual designs of 1000, 2000 and 3000 metric tons are examined at design speeds of 60, 80, and 100 knots.

DESCRIPTION OF LARGE CONCEPTUAL AIR CUSHION VEHICLES

The distinctive feature of the large conceptual ACV's that are examined here is a water propulsion system consisting of a number of identical strut-pod-propeller units that are mounted beneath the hard ACV structure. Fully submerged propellers are used for propulsion. Each strut-pod-propeller unit is powered by one engine. The number of units is determined by the powering and thrust requirements of the particular conceptual ACV. Retraction of the strut-pod-propeller unit may be achieved by swinging the unit transversely about the fore and aft axes of the right angle drive gears mounted in the top of the strut. This retraction arrangement is similar in concept to the retraction of the strut-pod-foil-propeller unit on the 320 ton AGEH-1 Hydrofoil boat.

The estimation of total required power for these large ACV conceptual designs involves:

1. bare ACV drag prediction
2. selection, sizing and performance estimation of suitable struts, pods, and propellers
3. selection of the power train arrangements and the sizing of gears and shafts

The bare ACV drag is defined as the force required to push an ACV configured without struts, pods or propellers. Bare ACV drags for 1000, 2000 and 3000 ton displacements at several length-beam ratios and cushion pressures at hump and design speeds of 60, 80, and 100 knots in Sea State 3 were supplied by R. Lebeau of the David W.

Taylor Naval Ship R&D Center, Code 1611. Using these drags as a starting point, the strut-pod size and drag was calculated along with propeller sizes and efficiency in an iterative manner in order to determine overall craft performance. The results of the first iteration are reported here.

SELECTION OF PROPULSION TRAIN ARRANGEMENTS

Prior to any hydrodynamic performance calculation, several propulsion train arrangements were investigated. Schematics of these arrangements are shown in Figures 1 through 5. Preliminary transmission design calculations were performed for each arrangement in order to determine minimum gear sizes and gear box envelopes. In all the arrangements, one FT-9 engine drives one strut-pod propulsion unit.

Taking into account the growth potential of FT-9 gas turbine engines, the following engine characteristics have been assumed for each arrangement.

Continuous Power 40,000 HP (29.8 MW)

Power Turbine Speed 4,000 RPM

40,000 HP corresponds to the maximum intermittent power of the present FT-9A-2 gas turbine which is in the developmental stage. Gearbox calculations were performed for a 40,000 HP engine output thus providing a desirable safety margin if a no-growth engine will be used. The total torque, T, transmitted by the engine at 4000 RPM is:

$$T = \frac{63025 \times \text{HP}}{n} = \frac{63025 \times 40,000}{4000} = 630250 \text{ lb. in. (71.20 KNm)}$$

Speed reduction can be accomplished in several ways. Figures 1 and 2 show the arrangements in which the rotational speed is reduced to the propeller speed in a helical gearbox between the strut and the engine. The arrangement similar to Figure 2 was used successfully in the transmission for the AGEH-1 hydrofoil. In the arrangements of Figures 3, 4, and 5 there is no reduction in the rotational speed of the vertical shafts transmitting power to the propeller. The speed reduction may be accomplished in a planetary with fixed ring gear, star planetary or multibranch concentric double reduction gearbox. The input and output shafts of these gearboxes are co-axial. Any off-set, parallel axes, gearbox will involve much greater sizes of the pod. The sizes of bevel gears for the arrangements of Figures 1 and 2, are calculated as shown in Table 1 for three assumed propeller RPMs. (See the Calculation of Main Sizes of Spiral Bevel Gearboxes section of this report.)

TABLE 1

Torques and Bevel Gear Diameters for the Arrangements of Figures 1 and 2

Propeller RPM	Figure 1 - Reduction at engine (single shaft)		Figure 2 - Reduction at engine (dual shaft)	
	Torque lb. in.	Bevel Gear Dia. in.	Torque lb. in.	Bevel Gear Dia. in.
750	3.3×10^6	50.9	1.65×10^6	40.3
1250	2.0×10^6	42.8	1.0×10^6	34.0
1750	1.4×10^6	38.4	0.7×10^6	30.4

The maximum diameter of the bevel gear which may be generated on the new bevel gear generator, manufactured by the Gleason Co., is 34 in. On the basis of the Table 1 we can see that a single shaft arrangement is impossible to build at the present. In the case of dual shaft arrangements with the reduction at the engine the lowest proposed rotational speed of the propeller, i.e., 750 RPM, cannot be realized. However the gearboxes with 30.4 and 34.0 in. diameter gears will be very heavy and involve very large pod dimensions. In Figures 3, 4, and 5 the speed reduction is in the pod. Figure 3 represents a single vertical shaft between upper and lower bevel gearboxes. Figure 4 shows a dual shaft arrangement. In the Figure 5 schematic, splitting of the torque is accomplished by means of two vertical concentric shafts. (See Ref. 1) Table 2 shows the characteristic data of bevel gears at the rotational speed of 4000 RPM.

We can see that the smallest bevel gear sizes may be obtained for the dual or concentric shafts. Pitch line velocity in the case of a single shaft exceeds the present state-of-art 25,000 ft/min limit. The bevel gear diameter for the single shaft arrangement, Figure 3, is within the capacity of the bevel gear generator but is much larger than the bevel gears in the dual shaft arrangement and therefore involves a heavier and larger gearbox. In addition, thrust on the horizontal shaft, on which the bevel gears are mounted, exceeds the capacity of existing thrust bearings.(Ref. 2) in the case of dual shafting, axial loads on bevel gears cancel each other. On the basis of Table

2 the dual shaft or concentric shafts arrangement are recommended. The latter arrangement involves a more compact and lighter design, however, is well outside the present state-of-art and requires extensive development work. The length of a bevel gearbox for concentric shafts is shorter, however the height of the gearbox becomes greater, since it must accommodate bearings under the lower bevel gear. The out-of-state-of-art condition and the larger height requirement of the concentric shaft arrangement dictated the dual shafting arrangement, Figure 4, for the selection.

TABLE 2

Characteristic Data of Bevel Gears at the Rotational Speed of 4000 RPM

	Torque lb. in.	Bevel Gear pitch dia. in.	Bevel Gear Pitch Line velocity
Single shaft (Figure 3)	630250	29.17	30,531
Dual Shafting or Concentric Shafts (Figures 4 and 5)	315125	22.71	23,770

DETERMINATION OF MINIMUM GEARBOX ENVELOPES

According to the selected power train arrangement of Figure 4 each pod houses one right angle bevel gear box and one reduction gearbox. The following calculations were performed to determine which of these gearboxes is larger in diameter. The larger gearbox determines the pod diameter. The following calculations for determining bevel gear box envelopes are at 40,000 HP and 4000 RPM engine speed.

Calculation of Main Sizes of Spiral Bevel Gearboxes

The bevel gear diameters shown in Table 1 and 2 have been calculated by equation (1):

$$d_p^3 = \frac{T N}{0.112 S_t J} \quad (1)$$

where, d_p = pitch diameter, in.

T = torque transmitted by one gear, lb. in.

N = number of teeth

S_t = bending stress at the root of the tooth, psi

J = geometry factor, (strength)

The above equation is valid for the gear ratio 1 to 1 and has been derived from the basic Gleason's expression(Ref. 2) for bending stress assuming:

Angle of pressure = 25°

Spiral angle = 25°

Overload factor $K_o = 1$

Dynamic factor $K_v = 1$

Size factor $K_s = 0.86$

Load distribution factor = 1.1

For configurations, Figures 4 and 5, the torque transmitted by one gear is equal to 315,125 lb. in. For calculation of the minimum pitch diameter the following assumptions were made:

$S_t = 30,000$ psi

$N = 50$, the corresponding value of the geometry factor $J = 0.400$

The allowable bending stress of 30,000 psi for bevel gears and the maximum contact stress of 200,000 psi require that AMS 6265 (9310 CEVM) steel carburized to a minimum surface hardness of $R_c 60$ be used.

The minimum pitch diameter of a bevel gear based on the criterion of durability becomes smaller for large gears than that calculated on the criterion of the tooth strength. Hence the determination of principal sizes of gears based on the latter criterion is fully justified.

Using the above mentioned data the pitch diameter for one spiral bevel gear used in configuration 4 or 5 is calculated to be:

$$d_p = \left[\frac{315,125 \times 50}{0.112 \times 30,000 \times 0.400} \right]^{1/3} = 22.7099 \text{ in. (580 mm)}$$

and the diametral pitch is:

$$P_d = \frac{N}{d_p} = \frac{50}{22.7099} = 2.2016 \text{ teeth/inch (module} = \frac{25.4}{P_d} = 11.53 \text{ mm)}$$

The metric sizes shown are standardized values according to I.S.O. standards. Figures 6 and 7 show the schematic of this gearbox.

Potential Rating

As experience is built up on a particular gearbox and gear design, a potential rating may be considered for an intermittent operation. This potential rating may be calculated for 35,000 psi bending stress or 250,000 psi contact stress according to Gleason Co. experience.

The potential power rating calculated for the above mentioned higher bending stress is equal to 47,930 HP for the bevel gearbox, i.e., about 20% higher than the nominal.

Principal sizes of reduction Gearbox Between the Lower Bevel Gearbox and the Propeller

For three assumed propeller speeds, reduction ratios are shown in Table 3. Minimum gearbox envelopes for each of these gearboxes have been estimated.

TABLE 3

Reduction Ratios for Assumed Propeller Speeds

Propeller Speed RPM	Reduction Ratio $\frac{m}{g}$
750	5.333
1250	3.200
1750	2.285

Reduction Gearbox for Ratio $m_g = 5.333$

In a planetary gearbox that may be designed for the above ratio the critical component is the sun gear. The minimum sun gear diameter may be calculated by equation (2), (Ref. 3) which is based on the condition of durability.

$$d_s = 50 \left[\frac{1}{bK} \times \frac{P_s}{n_s} \times \frac{m_g}{m_g - 2} \right]^{1/3} \quad (2)$$

Where, d_s = sun gear pitch diameter, in.

b = number of planets

K = durability factor

P_s = total power transmitted by the sun gear

n_s = RPM of the sun gear

The above equation is based on the assumption that the face width of the sun gear is equal to pinion diameter. For double helical gears which will be applied in our planetary gearbox the face width may be greater, and may reach the double pinion diameter. For the reduction ratio = 5.333 the number of planets cannot be greater than 4. (Reference 3) The K factor will be assumed equal to 500. This value is much higher than that used in conventional marine gearing, however, a K factor greater than 500 has been used successfully by the British. In helicopter technology, K factors on the order of 1000 have been used for years.

Using formula (2) the sun gear pitch diameter d_s is:

$$d_s = 50 \left[\frac{1}{4 \times 500} \times \frac{40,000}{4,000} \times \frac{5.33}{3.33} \right]^{1/3} = 10.005 \text{ in.}$$

and the ratio of the ring gear to sun gear diameter $\frac{d_r}{d_s}$ is

$$\frac{d_r}{d_s} = m_g - 1 = 4.333$$

The ring gear diameter d_r becomes

$$d_r = 4.333 \times 10 = 43.33 \text{ in.}$$

and the planet pitch diameter d_p is:

$$d_p = \frac{43.33 - 10}{2} = 16.66 \text{ in.}$$

To determine the number of teeth the diametral pitch in the transverse plane should be calculated by equation (3) by assuming the bending stress at the root of the tooth is 45,000 psi. (The allowable bending stress using 9310 CEVM steel carburized to a minimum surface hardness of $R_c = 60$ is equal to 50,000 psi). We assume double helical gears with angle of pressure $\phi = 20^\circ$ and helix angle $\psi = 30^\circ$. The basic equation for the bending stress:

$$S_t = \frac{W_t \times K_o}{K_v} \times \frac{P_d}{F} \times \frac{K_s K_m}{J} \quad (3)$$

Where, W_t = tangential load

P_d = diametral pitch in transverse plane

K_o = overload factor, (assumed = 1.25)

K_v = dynamic factor, (assumed = 1)

K_s = size factor, (assumed = 1)

K_m = load distribution factor, (assumed = 1.4)

F = width of gear (assumed equal to d_s)

The average value of J may be assumed = 0.46 (see Figure 17, AGMA 226.01) (Reference 4). After the number of teeth is determined the corrected value of J will be found.

Solving equation (3) for P_d we have

$$P_d = \frac{S_t \times F \times J \times K_v}{W_t \times K_o \times K_s \times K_m}$$

$$W_t = \frac{2T}{d_s b} = \frac{2 \times 630250}{10 \times 4} = 31,512 \text{ lb}$$

$$P_d = \frac{45,000 \times 10 \times 0.46 \times 1}{31,512 \times 1.25 \times 1.4} = 3.753$$

The number of teeth in the sun gear, N_s , is:

$$N_s = P_d \times d_s = 3.75 \times 10 = 37.5$$

Assuming $N_s = 36$ the exact value of P_d is:

$$P_d = \frac{36}{N} = 3.6$$

and the normal diametral pitch is:

$$P_{d_n} = \frac{P_d}{\cos 30^\circ} = \frac{3.6}{.886} = 4.156$$

and the number of teeth in the ring gear, N_r , is:

$$N_r = 36 \times 4.333 = 155.98 \approx 156$$

Number of teeth in the planet gear, N_p , is then:

$$N_p = \frac{N_r - N_s}{2} = \frac{156 - 36}{2} = 60$$

In order to assemble the gearbox, $(N_s + N_r)$ must equal $N_p \times I$ where I is any integer. For the above gearbox $I = (36 + 156)/4 = 48$.

Given the number of teeth the corrected value of the geometry factor J may be found and the corrected bending stress may be calculated. Using Figures 17 and 23 from Reference 4, the J factor may be taken equal to 0.45. Using this value and the corrected P_d the stress S_t becomes:

$$S_t = \frac{31,512 \times 1.25 \times 3.6 \times 1 \times 1.4}{10 \times 0.45} = 44110 \text{ psi}$$

The metric sizes of the reduction gearing are expressed in terms of a module.

The module in normal plane is $m_n = \frac{25.4}{P_{d_n}} = \frac{25.4}{4.156} = 6.11 \text{ mm}$

The nearest standardized value, $m_n = 6$, has been assumed.

The module in transverse plane is $m = \frac{m_n}{\cos 30} = \frac{6}{0.866025} = 6.9282 \text{ mm}$

The exact value of the diametral pitch is $P_d = 25.4/6.9282 = 3.666$

and the exact gear pitch diameters are:

$$d_s = 36 \times 6.9282 = 249.415 \text{ mm}$$

$$d_r = 156 \times 6.9282 = 180.800 \text{ mm}$$

$$d_p = 60 \times 6.9282 = 415.692 \text{ mm}$$

The bearings which support planet gears may pose a special problem because in addition to tooth loads they are subjected to very large centrifugal forces which may be of the order of the magnitude of the gear tooth forces. The additional centrifugal forces would rule out the use of rolling element bearings and require that hydrodynamic sleeve bearings be used.

The lubrication of hydrodynamic sleeve bearings becomes a severe problem, and indeed lubrication problems were encountered during the development of a 40,000 HP experimental planetary reduction gearbox built by Curtiss-Wright. For gear ratio 5.333 the problem may be even more severe, because the planets are much larger than in the Curtis Wright gearbox and centrifugal forces are much greater.

Assuming that the mass of the planet gear is concentrated at the planet center line, the centrifugal force, F, is:

$$F = \frac{W}{g} \times r \times \left(\frac{2\pi n}{60}\right)^2$$

where, W = weight of the planet gear

$$g = 32.2 \text{ ft/sec}^2$$

r = radius to the planet center line = 13.18 in.

n = carrier RPM = 750.

The diameter of the planet bore has been assumed equal to 8" and the length of the shaft is assumed to be 11 in. to allow for the recess between left and right hand helical gears.

The weight of the solid gear is about 520 lb. By recessing the gear faces it may be reduced by 50%. For an assumed gear weight, W = 260 lb, the centrifugal force is then calculated to be:

$$F = \frac{260}{32.2} \times \frac{13.18}{12} \times \left(\frac{2\pi \cdot 750}{60}\right)^2 = 54,647 \text{ lb.}$$

A vector diagram of the previously calculated tangential load, $W_t = 31,512 \text{ lb.}$ is shown in Figure 8. According to this diagram, the resultant force acting on the sleeve bearing is approximately

101,200 lb., and the unit pressure p in the sleeve bearing is:

$$p = \frac{101,200}{8 \times 11} = 1150 \text{ psi.}$$

This pressure is high and requires a steel backed leaded bronze in the bearing and an oil with a viscosity selected for this pressure.

Figure 9 shows the schematic arrangement of the planetary gearbox and thrust bearing. With a ring gear diameter of 43.3", the outside diameter of the gearbox is approximately 51" = 1300 mm.

The Kingsbury thrust bearing size is estimated by assuming that the maximum static pressure between the thrust shoes is 350 psi (241 N/cm²). For a maximum thrust of 600 KN and a 10 inch (25.4 cm) propeller shaft the thrust bearing diameter becomes 61 cm. The minimum diameter required for fitting the thrust bearing in the pod is less than the diameter of the planetary gear envelope.

Reduction Gearbox for Ratio $m_g = 3.2$

The minimum sun gear diameter can be assumed equal to 10 in. as in the case of the 5.33 reduction ratio gearbox. For the planetary unit with rotating carrier as the critical shaft, the ring diameter is

$$d_r = d_s (m_g - 1) = 10 \times 2.2 = 22 \text{ in.}$$

and the planet gear diameter is $d_p = \frac{22-10}{2} = 6 \text{ in.}$ Evidently a planetary gearbox with rotating carrier cannot be built because the planet gear diameter becomes only 6". The durability condition requires minimum

10 in planet diameter. In addition the planet shaft will be too small to allow for attainable bearing pressure. However, a star planetary reduction gearbox may be considered. Assuming that the sun gear pitch diameter is equal to 10 in. as in the case of the 5.33 reduction ratio gearbox, the pitch diameter of the rotating ring gear is

$$d_r = d_s \times m_g = 10 \times 3.2 = 32 \text{ in.}$$

The stresses due to tooth loads will be comparable with the planetary units if the number of planets is assumed to same, i.e., equal to 4. Consequently, the diametral pitch for gears and the number of teeth in the sun gear may be assumed the same as in the 5.33 reduction ratio gearbox.

One of the advantages of a star planetary gearbox is the absence of centrifugal forces since the planets are rotating about fixed centers. Hence the problems associated with lubrication of planet shaft bearings vanish.

Assuming the number of teeth in sun gear is equal to $N_s = 36$, the number of teeth in the ring gear is

$$N_r = 36 \times 3.2 = 115.2$$

$N_r = 116$ must be assumed, giving the actual reduction ratio $\frac{116}{36} =$

3.22. The diametral pitch in transverse plane is

$$P_d = \frac{36}{10} = 3.6$$

and the number of teeth in the planet gear is

$$N_p = \frac{116 - 36}{2} = 40.$$

The corrected ring diameter is

$$d_r = \frac{N_r}{P_d} = \frac{116}{3.6} = 32.22.$$

and the pitch diameter of the planet gear is

$$d_p = \frac{40}{3.6} = 11.11 \text{ in.}$$

Since the diametral pitch in the transverse plane has been assumed 3.6, i.e., the same as in the planetary 5.33 reduction ratio gearbox, the metric module governing the sizes of gears will be also identical for the same helix angle of 30°.

For the module in the transverse plane equal to 6.9282 mm the exact gear pitch diameters are:

$$d_s = 36 \times 6.9282 = 249.415 \text{ mm}$$

$$d_r = 116 \times 6.9282 = 803.671 \text{ mm (31.64 in.)}$$

$$d_p = 40 \times 6.9282 = 277.128 \text{ mm}$$

The ring gear with a 31.64 inch gear pitch diameter will have an outside diameter of 34 inches. The envelope of the gearbox may be estimated to be 36 in. (915 mm). The schematic of the planetary-star arrangement is shown in Figure 10.

Reduction Gearbox for Ratio $m_g = 2.285$

The planetary gearbox with stationary ring gear is here ruled out as in the case on the 3.2 reduction ratio gearbox. A star planetary reduction gearbox will be considered. It will be shown that, inherent for the above ratio, small diameter planet gears are highly loaded and a development work must be provided to verify experimentally the new design.

Alternatively, a multibranch concentric double reduction gearbox may be provided, but the component gears are expected to be much greater than those of the star-planetary gearbox. Consequently,

the gearbox envelope is expected to be greater. Development work will be indispensable, since no multibranch concentric double reduction gearboxes transmitting 40,000 HP have been built.

Six planets may be used in a star planetary gearbox with a reduction ratio of 2.285. Hence, the minimum pitch diameter of the planet gear will be smaller than in the 5.33 and 3.2 reduction ratio gearboxes. The minimum sun gear pitch diameter will be assumed the same as before, i.e., 10 in. since the input shaft connected to the sun gear will transmit the same torque.

The ring gear diameter is

$$d_r = 10 \times 2.285 = 22.85 \text{ in.}$$

and the planet gear pitch diameter is

$$d_p = \frac{22.85 - 10}{2} = 6.43 \text{ in.}$$

Assuming the number of sun gear teeth, $N_s = 36$, as before, the number of ring gear teeth, N_r , becomes

$$N_r = 36 \times 2.285 = 82.26$$

$N_r = 84$ will be assumed, and the actual ratio becomes

$$m_g = \frac{84}{36} = 2.333$$

The number of teeth in the planet is

$$N_p = \frac{84 - 36}{2} = 24$$

and the corrected ring gear and planet gear pitch diameters are:

$$d_r = 10 \times 2.333 = 23.33 \text{ in.}$$

$$d_p = \frac{23.33 - 10}{2} = 6.665 \text{ in.}$$

The transverse plane diametral pitch, the transverse plane module and the helix angle values of the 2.285 reduction ratio gearbox are the same as those of the 5.33 and 3.22 reduction ratio gearboxes.

The exact gear pitch diameters are calculated to be:

$$d_s = 36 \times 6.9282 = 249.415 \text{ mm}$$

$$d_r = 84 \times 6.9282 = 581.968 \text{ mm (22.91 in.)}$$

$$d_p = 24 \times 6.9282 = 166.276 \text{ mm}$$

To check the minimum pitch diameter of the planet gear on the basis of required durability equation (4) may be applied. In this case we can consider the planet gear as the pinion and we use the actual RPM of the planet gear. We assume also that the load is uniformly carried by all planets.

Using the above mentioned equation we have:

$$d_p^2 = \frac{12.6 \times 10^4}{FK} \times \frac{P}{b} \times \frac{1}{n_p} \times \frac{m_g + 1}{m_g} \dots \quad (4)$$

where, b = number of planet gears = 6.

$$m_g = \frac{d_s}{d_p} = \frac{10}{6.665} = 1.5$$

P = power

$$n_p = 6000 \text{ RPM}$$

$$F = d_s = 10 \text{ in. (this face width should be the same as for the sun gear.)}$$

$$d_p = \left[\frac{12.6 \times 10^4}{10 \times 500} \times \frac{40,000}{6} \times \frac{1}{6000} \times \frac{2.5}{1.5} \right]^{1/2} = 6.8 \text{ in.}$$

The 6.8 in. planet gear pitch diameter is sufficiently close to the actual 6.665 in. value previously calculated. The lubrication of the planet gear bearings may be a problem.

The tangential load transmitted by the sun gear to the planet gear is:

$$W_t = \frac{2T}{d_s \times b} = \frac{2 \times 630,520}{10 \times 6} = 21,000 \text{ lb.}$$

The normal force to the tooth surface is:

$$W_{tn} = \frac{21,000}{\cos 20} = 22,350.$$

The same force is exerted by the ring gear hence the total load on the sleeve bearing supporting the shaft is 44,700 lb.

Assuming a shaft diameter of 3 in., and a bearing length of 11 inches, the unit bearing pressure, P, is then calculated.

$$p = \frac{44,700}{3 \times 11} = 1355 \text{ psi}$$

This pressure is higher than in the 5.33 reduction ratio gearbox, hence the lubrication problem may be serious.

Multi-Branched Concentric Double-Reduction Gearbox for the Reduction Ratio 2.285

A multi-branched concentric double-reduction gearbox will be discussed as an alternative solution. Schematic of this reduction gearbox is shown in Figure 11. The number of branches will be assumed equal to 4, and the pitch diameter of the input pinion equal to 10 in.

The total reduction ratio can be split evenly between two stages, therefore the gear ratio for each stage will be equal to the square root of 2.285 or approximately 1.5. The pitch diameter d_g of the driven gear in each stage is: $d_g = 10 \times 1.5 = 15 \text{ in.}$

The speed of the second reduction pinion is $N_p = \frac{4000}{1.5} = 2,666$ RPM and the torque transmitted by the pinion of second stage for each branch is:

$$T = \frac{63,025 \times 10,000}{2,666} = 236,402 \text{ lb. in.}$$

Since the torque transmitted by the second stage is greater than that associated with the first one, the face width of the pinion must be increased if the pinion diameter has to be the same as for the first stage, i.e., 10 in.

The required face width will be calculated using equation (4):

$$F = \frac{12.6 \times 10^4 \times 40,000 \times 2.5}{10^2 \times 4 \times 2666 \times 500 \times 1.5} = 15.74 \text{ in.}$$

The bending stress at the root of the tooth should be checked using equation (3). The diametral pitch is 3.6 and the number of teeth in the pinion is 36. The tangential load $W_t = \frac{236,402}{10/2} = 47280$ lb. and the tooth bending stress S_t is:

$$S_t = \frac{47280 \times 1.25}{1} \times \frac{3.6}{15} \times \frac{1 \times 1.4}{0.45} = 44,128 \text{ psi.}$$

The diameter of gears envelope D as shown in Figure 11 is given by equation (5)

$$D = d_s + 2 \times d_g + 2a = 10 + 2(15) + 2(.28) = 40.56 \text{ in.} \quad (5)$$

where, d_g = pitch diameter of the gear in the first stage

$$a = \text{addendum} = \frac{1}{P_d} = \frac{1}{3.6} = 0.28.$$

The housing outside diameter is estimated to be 45 in. (1150 mm).

On the basis of the foregoing discussion on the arrangement of planetary reduction gearbox for various gear ratios we may conclude

that for small reduction ratios the small pitch diameter of the planet member involves problems with planet tooth strength and with lubrication of the bearings supporting the planet gear shafts. For the higher ratios a large diameter of the planet gear involves problems associated with centrifugal force, causing additional loads in the bearings. For the star planetary arrangements the large centrifugal force problem does not exist, however the gearbox envelope is greater for the star arrangement than for the same reduction ratio planetary unit with stationary ring gear. For a planetary unit with stationary ring gear the optimum condition, from a planet gear durability point of view, can be obtained when sun gear diameter is equal to planet gear diameter. In this case, the gear reduction ratio is equal to 4. A reduction gearbox transmitting 40,000 HP with reduction ratio 4 to 1 has been developed by the Curtiss-Wright Co. and its envelope is 36 in. Table 4 shows the estimated envelopes of the 5.33, 3.2 and 2.285 reduction ratio gearboxes as well as the 4.0 reduction ratio gearbox and the right angle bevel gear unit.

It should also be noted that, with exception of the reduction ratio 5.333 to 1, the sizes of the lower bevel gearbox govern the pod diameter. The arrangements of Figures 3, 4, and 5, as compared to the arrangements of Figures 1 and 2 involve smaller pod diameters at the expense of greater pitch line velocities. In some publications the capacity of gearing is often quoted in terms of power per mesh. This is rather misleading, since it should be expressed in torques per mesh at the associated pitch line velocity. Table 5 shows a comparison of the AG(EH) - 1 gearbox with the designs developed in

ENGINE POWER = 40,000 HP (29.8 MW)
 ENGINE SPEED = 4,000 RPM

REDUCTION GEARS		ESTIMATED DIAMETER OF GEARBOX ENVELOPE CM.
RATIO	TYPE	
5.33	PLANETARY - RING GEAR STATIONARY	130
4	PLANETARY - RING GEAR STATIONARY	92
3.2	PLANETARY - STAR	92
2.285*	PLANETARY - STAR	77
2.285*	MULTI-BRANCH CONCENTRIC DOUBLE REDUCTION	115
RIGHT ANGLE BEVEL GEAR - DUAL MESH		102

*OUTSIDE S.O.A. NEED EXTENSIVE DEVELOPMENT

Table 4 - Estimated Envelope of Gearboxes

	HP/MESH	TORQUE/MESH lb. in.	PITCH LINE VELOCITY ft/min
AG(EH-1)	7,500	380,000	8,000
AC-ACV	20,000	315,025	24,000

Table 5 - Capacities of Spiral Bevel Gears

this report. We can see that HP/mesh for AG(EH) - 1 is lower, but torque/mesh is higher. However the pitch line velocity of the AG(EH) - 1 bevel gear is much lower than the pitch line velocity of our gearboxes. The high pitch line velocities may cause problems in the marine applications considered here. Although the Gleason Co. considers that 25,000 ft/min for the spiral bevel gearing is within the present state-of-art, no marine transmission has been operated successfully while transmitting high order powers at this pitch line velocity. An experimental spiral bevel gearbox transmitting 40,000 HP at 4,000 RPM was built by the Gleason Co. in 1963-64, but a casualty occurred after 40 hours of run. Casualty investigations revealed that some improvement in design and metallurgical areas would contribute to a successful result, but the transmission was never rebuilt. Consequently, considerable development work should be expected for the future 40,000 HP bevel gearboxes.

High pitch line velocities cause a rapid temperature rise leading to oil film breakdown, scoring, and thermal distortions of the teeth. Maag Co., who built one of the largest reduction units in the world, with helical gears of the capacity 85,000 HP/mesh, 1.8×10^6 lb in. torque per mesh at 27,000 ft/min pitch line velocity, has found that the temperature rise is nearly all speed dependent. With no load on the unit the temperature of the pinion increased rapidly with speed from 40°C to approximately 160°C at the hottest zone. After the full load was applied the temperature rose only few degrees.

In order to account for the effects of thermal deflections and to assure a uniform load distribution across the face, all high speed

pinions and some high speed gears have to be ground with longitudinal corrections. It will be necessary to establish the proper longitudinal corrections for the 40,000 HP high pitch line velocity gears discussed in this report.

DETERMINATION OF MINIMUM STRUT THICKNESS AND POD DIAMETER

The diameter of the vertical shafts in the dual shaft arrangement can be estimated by assuming that the shearing stress is about 12,000 psi. This assumption is rather conservative for a high strength steel such as MIL-S-23284, but takes care of the neglected bending and alternate stresses. The required section modulus of the shaft is equal to $T/S_s = (315,125/12,000) = 26.2 \text{ in}^3$. The corresponding required shaft diameter is 5 in. (127 mm).

All of the previous gear size calculations culminating in the results presented in Table 4 are for an assumed 4000 RPM engine speed. They show that it is reasonable to design for 40,000 HP per propulsion unit. Many of the conceptual ACVs examined in this report did not utilize the full 40,000 HP at design speed and therefore a quicker method of estimating gear and shaft sizes was needed. Figures 12 and 13 from Reference 5 were spot checked and adopted for use in this report.

The minimum strut shaft diameter, obtained by extrapolation, using Figure 12 (40,000 HP, 4000 RPM) is 165 mm which is more conservative than the previously calculated 127 mm. Nevertheless the result from Figure 13 was used. The minimum thickness of the strut can be determined

by allowing space for the strut bearings and strut shell thickness. A conservative approach for determining minimum strut thickness is to assume that the outside diameter of the bearings and coupling is 2.5 times the shaft diameter and to allow a small additional distance for the strut skin thickness. However, Reference 5 uses an overall strut thickness of 2.0 times the shaft diameter and Reference 8 uses a figure of 2.15 in their sample case. In all likelihood, the ratio of minimum strut thickness to shaft diameter will be greatly dependent on detailed design.

In this report, a ratio of 2.25 was chosen for all calculations and the 4,000 RPM curves of Figures 12 and 13 were combined to yield the following strut thickness expression:

$$\text{strut thickness}_{\text{(at base)}} = \left[\frac{\text{max. pod dia.}}{3} + .03 \right] \text{ meters.}$$

It should be noted that this strut sizing method neglects the hydrodynamic side loads on the strut. For certain configurations and maximum design speeds, the minimum strut section modulus needed to overcome bending loads may require a thicker strut than dictated by minimum space requirements.

PROPELLER SELECTION AND PERFORMANCE

Semi Submerged Propellers

The initial large ACV concept used semi submerged propellers. Because of the following four reasons, the use of semi submerged propellers was discarded.

1. The waterline under an ACV varies with forward speed, water depth, and craft motions. Operating a semi submerged propeller without a steady waterline would be very difficult.
2. A large ACV yaw angle would result in large propeller blade shock loading as the semi submerged propeller blades re-enter the water.
3. Semi submerged propellers create large side forces which would be a problem in the design of retractable strut-pod units.
4. Semi submerged propellers operate with a large rooster tail which, for a propeller mounted beneath the cushion, would impinge on the ACV hard structure or skirt and cause an additional drag.

Fully Submerged Supercavitating Propellers

Preliminary propeller calculations indicated that the controllable pitch feature of a propeller was advantageous for use on the large ACV conceptual designs. The 100 knot speed (cavitation number, $\sigma = 0.096$) requirement limited the selection to propellers which have been tested at a very low cavitation number. Controllable pitch propeller characteristics over a cavitation number range corresponding to hump speed (12 to 17 knots depending on the ACV) and maximum design speed of 100 knots were not available and therefore two fixed pitched propellers were selected to represent a controllable pitch propeller. The geometric characteristics of these propellers are presented in Table 6.

TABLE 6 - Propeller Geometry

Propeller	DTNSRDC 3767	DTNSRDC 3785
No. of blades	3	3
Pitch-diameter ratio	1.18	1.61
Expanded area ratio	0.506	0.457

The open water efficiency and thrust coefficient in K_T/J^2 form for propeller 3767 are presented in Figure 14. The $\sigma = 2, 3, 4, 5, 6,$ and 7 results are cross faired from the experimental results at $\sigma = 1.68, 4,$ and 7 as reported in Reference 6. Figure 14 is used to estimate the open water performance of the propeller at hump speed.

The open water characteristics of propeller 3785 for design speeds of 60, 80 and 100 knots are presented in Figures 15, 16 and 17. These data are based upon experimental results at cavitation number of 0.5, 0.2 and 0.1465 as presented in Reference 6. The 100 knot condition is extrapolated, and the 60 knot condition is interpolated. While these two propellers do not represent the performance that would be available with a controllable pitch design, they should yield predictions which are acceptable for this preliminary investigation. It is expected that a pitch optimized design would yield slightly different diameter propellers operating at different RPMs. The maximum attainable efficiency of a pitch optimized design is not expected to be significantly higher than the efficiencies shown in Figures 15, 16 and 17.

HYDRODYNAMIC STRUT-POD DESIGN AND PERFORMANCE

A superventilated strut and pod were chosen because of the high (60, 80 and 100 knot) design speeds. The pod design of Reference 5 was adopted for this report. The pod is a one term modified paraboloid with a base diameter equal to .707 maximum diameter. The strut sections are base vented, one term modified parabolas with zero trailing edge slopes. The geometric characteristics of the strut pod designs are given in Table 7.

Total strut drag is assumed to be the sum of friction drag and base drag. Form drag is assumed to be zero. The Schoenherr friction coefficient is used to estimate friction drag on the strut wetted area. The strut base drag coefficient is taken as $C_{DB} = \frac{9\pi}{128} (t/c)$ from Reference 5. Figure 18 presents predicted strut drags for the 60, 80 and 100 knot designs as a function of pod maximum diameter.

The drag of the pod is also assumed to be the sum of friction drag and base drag. Form drag is assumed to be zero. The Schoenherr friction coefficient is used to predict friction drag on the wetted areas presented in table 7. The pod base drag coefficient is assumed to be $C_{DB} = .14(d/\ell)^{.15}$. (See Reference 7.) Calculated pod drags for the 60, 80 and 100 knot designs are presented in Figure 19.

It should be emphasized that the strut base drag coefficient is a theoretical value shown in Reference 5 and that the pod base drag coefficient is an approximation to the theory of V. Johnson as formulated by Hoerner. In addition, strut-pod interference drag is not considered. It is expected that these drag predictions are optimistic.

PERFORMANCE ESTIMATES FOR POINT DESIGNS

Powering performance estimates for 1000, 2000 and 3000 metric ton ACVs were made. Design speeds of 60, 80 and 100 knots were specified for each displacement. The following algorithm shows the steps used in the performance prediction.

Table 7 - Strut Pod Geometry

DESIGN SPEED KNOTS	STRUT CHORD TO THICKNESS RATIO (c/t)	POD LENGTH TO DIAMETER RATIO (ℓ/d)	POD WETTED SURFACE COEFFICIENT M
60	3.1	3.0	1.06
80	5.6	4.3	1.09
100	8.7	6.4	1.02

c = STRUT CHORD
 t = STRUT THICKNESS
 ℓ = POD LENGTH
 h = STRUT IMMERSSED DEPTH
 d = POD MAXIMUM DIAMETER
 M = POD WETTED SURFACE COEFFICIENT

POD WETTED SURFACE = $M\pi d\ell$
 STRUT WETTED SURFACE = $2hc$

Performance Prediction Algorithm:

Given: displacement, design speed; craft length-beam ratio L/B, cushion pressure P_c/\sqrt{s} , sea state, no. of propellers

1. Determine bare ACV drag at design speed (S.S 3) and hump from Code 1611 computer output. Add 20% margin to computer predicted hump drag as suggested by Code 1611.
2. Assume a strut-pod drag at design speed. Total thrust required at design speed is equal to the sum of the strut pod drag and bare ACV drag.
3. For various propeller diameters calculate $T/\rho V^2 D^2$. Using the relationship
$$\frac{T}{\rho V^2 D^2} = K_T/J^2$$
and Figures 15, 16, and 17 as appropriate, determine open water propeller efficiency, RPM and required shaft power. Select propeller diameter.
4. Using Figure 13 determine pod diameter.
5. Using Figure 18 and 19 determine strut and pod drag.
6. Compare the strut pod drag as determined from step five to the assumed value in step two. Repeat steps two through five, adjusting the assumed pod drag value until agreement is reached between the assumed value and the calculated value.
7. Check if propeller produces sufficient thrust at hump using Figure 14. If insufficient hump thrust is produced, calculate minimum propeller diameter iterate through steps 2-6 for that minimum diameter. Calculate required power at hump.

In order to facilitate calculations, a small computer program was written to provide tabulated values of open water propeller efficiency, advance coefficient, RPM, K_T/J^2 and shaft power for small thrust increments and propeller diameters. The tables were based on Figures 15, 16 17.

Performance Assumptions

1. Thrust deduction = 0, wake fraction = 1, hull efficiency = 1 at 60, 80 and 100 knots. The required thrust is equal to the base ACV drag + strut + pod drag at hump. The required hump thrust is equal to 1.2 x bare ACV drag. (The drag of the pod at the low hump speed was calculated to be very small and was subsequently neglected.)
2. Propeller P/D=1.61 at 60, 80 and 100 knots.
3. Propeller P/D=1.18 at hump speed.
4. The pod diameter is dictated by the right angle bevel gear envelope. This assumption holds except for the 5.33 reduction ratio gearbox (See Table 4).
5. One engine drives one propeller; maximum continuous power available is 40,000 HP (29.8 MW) per engine.
6. Pod drag = base drag + friction drag.
7. Strut drag = base drag + friction drag.

The performance at hump and at design speed for the various conceptual designs is shown in Tables 8, 9 and 10. The thrust power required to thrust power available ratio at design speed is based on the projected continuous 29.8 MW power per engine at 4000 RPM. Engine characteristics at reduced RPM were not received, and therefore an assumed maximum intermittent power curve shown in Figure 20 was constructed using the method of Reference 8. In this method, normalized average gas turbine characteristics are curve fitted. The normalized power vs RPM curve is shown in the insert of Figure 20. The hump power required to hump power available ratio is based on the intermittent power curve of Figure 20.

The drag values in Tables 8, 9 and 10 are the sum of the ACV bare drag and the strut-pod drag. Inherent in the strut-pod sizing

Table 8 - Predicted Performance of 1000 Ton Concepts

1000 TON ACV $L/B=2.5 P_c/\sqrt{S} = 350 N/M^3$	SPEED	TOTAL DRAG KN	TOTAL POWER KW	PROPELLER DIA CM	PROPELLER RPM N	PROPELLER EFF. η_p	POWER REQUIRED POWER AVAILABLE from 29.8 MW engine
100 KNOT DESIGN 3 propeller; 3 engines max pod dia = 79 cm	100	1020	77,500	178	1428	.67	.87
	HUMP	900	23,000	178	700	.27	.30 @1960 RPM
		Reduction ratio = 2.8					
2 propeller; 2 engines max pod dia = 120 cm	100	980	74,000	211	1212	.67	1.25
	HUMP	900	24,000	211	640	.26	.46 @2112 RPM
		Reduction Ratio = 3.3					
At 100 knots, the 2 engine design requires more power than available.							
80 KNOT DESIGN 2 propeller; 2 engines max pod dia = 79 cm	80	684	42,000	211	990	.67	.73
	HUMP	900	24,000	211	640	.26	.40 @2585 RPM
		Reduction Ratio = 4.04					
60 KNOT DESIGN 2 propeller; 2 engines max pod dia = 65 cm	60	570	27,000	211	715	.67	.45
	HUMP	900	24,000	211	640	.26	.36 @3557 RPM
		Reduction Ratio = 5.59					
1 engine, 1 propeller needs a minimum propeller diameter of 3.74 cm and 31.5 MW of power at hump. - Design not pursued.							

Table 9 - Predicted Performance of 2000 Ton Concepts

2000 TON ACV L/B=2.5 $P_c/\sqrt{s} = 350 \text{ n/M}^3$ Note: 40,000 HP = 29.8 MW	SPEED	TOTAL DRAG KN	TOTAL POWER KW	PROPELLER DIA CM	PROPELLER RPM N	PROPELLER EFF η_0	POWER REQUIRED POWER AVAILABLE from 29.8 MW engine
100 KNOT DESIGN 4 propeller; 4 engine	100	1724	131,000	195	1315	.68	1.10
	HUMP	1810	52,000	195	767	.28	.46 @2333
10% more power is required than available from 29,800 KW engine max pod dia = 110 cm; Gear design outside S.O.A.; Reduction Ratio = 3.04							
80 KNOT DESIGN 3 propeller; 3 engines	80	1233	79,000	226	910	.67	.88
	HUMP	1810	55,500	226	703	.26	.58
max pod dia = 94 cm; Reduction Ratio = 4.39 2 engine; 2 propellers requires 38,000 KW per engine just to overcome bare ACV drag. - Design not pursued.							
60 KNOT DESIGN 3 propeller; 3 engines	60	1083	50,200	226	686	.67	.57 @3896
	HUMP	1810	55,500	226	703	.26	.54 @4000
max pod dia = 68 cm; Reduction Ratio (based on hump rpm) = 5.68							
2 propeller; 2 engines	60	1090	51,000	276	600	.67	.86
	HUMP	1810	55,500	276	590	.26	.81 @3900
Propeller diameter based on minimum diameter needed for hump thrust, power to overcome hump drag needs attention. max pod dia = 91 cm; Reduction = 6.66; The reduction of 6.66 is unrealistically large. A 4.0 reduction would result in 2360 hump RPM and the available 26.8 MW per engine results in a power required to power available ratio of 1.03							

3000 TON ACV L/B=3 $P_c/\sqrt{s} = 300 \text{ N/M}^3$	SPEED	TOTAL DRAG KN	TOTAL POWER KW	PROPELLER DIA CM	PROPELLER PRM N	PROPELLER EFF η_o	POWER REQUIRED POWER AVAILABLE from 29.8 MW engine
100 KNOT DESIGN 6 propellers; 6 engines max pod dia = 103 cm;	100 HUMP	2460 2070	187,000 54,000	178 178	1475 790	.68 .34	1.04 .34 @2138 RPM
80 KNOT DESIGN 4 propellers; 4 engines max pod dia = 102 cm;	80 HUMP	1840 2070	115,000 61,000	211 211	1040 723	.66 .30	0.96 .49 @2780 RPM
60 KNOT DESIGN 3 propeller; 3 engine max pod dia = 92 cm;	60 HUMP	1590 2070	76,000 68,000	239 239	727 677	.65 .27	.85 .66 @3724 RPM

Table 10 - Predicted Performance of 3000 Ton Concepts

is the assumption that the spiral bevel gearbox governs the minimum pod diameter as shown in Table 4. This assumption is certainly true for reduction ratios from 2.285 to 4 and for a value just larger than 4 but much less than 5.33. However, some of the resultant reduction ratios required as shown in Tables 8,9 and 10 are much larger than 4, and therefore violate the assumption that the bevel gearbox governs the pod size. There are several approaches to resolving this mismatch of assumed reduction ratio vs calculated - they are to:

- a) iterate for the required reduction ratio @ 4000 RPM of the downshafts
- b) set the reduction ratio at a maximum 4.0 in the hub and check to see if the engine produces sufficient power at off design powers
- c) consider a second reduction gearbox located between strut and engine
- d) adjust propeller pitch diameter to accommodate a maximum 4 to 1 reduction

All of these options point out the need for a computerized optimization technique because they involve extensive calculations. It is the opinion of the author that adjustment of the propeller pitch-diameter ratio would eliminate the mismatch between assumed reduction and resultant reduction.

Note that the resultant reduction ratios for the 80 knot designs, 4.04, 4.39 and 3.89 are all very close to the optimum ratio of 4. General propeller characteristics indicate that an increase in pitch diameter ratio moves the maximum propeller efficiency to a high operating J. A slight adjustment in propeller P/D could move all of the 80 knot reduction ratios to 4.0.

In the case of the 100 knot designs the propeller P/D should be increased above 1.61. The maximum efficiency would not change significantly, but the operating J would increase and the RPM would decrease to 1000 RPM range. The present 1428, 1315 and 1475 RPM for the 1000 knot designs could be accommodated by gear boxes that require extensive development, however, the high RPMs would result in high propeller blade stresses and pitch line velocities.

In the case of the 60 knot designs it would be extremely desirable to eliminate the large 5.59, 5.68 and 5.50 reduction ratios since these would result in excessively bulky pods, where diameters are governed by reduction gear space required instead of bevel gear space required. The extra bulk causes excessive pod drag. A downward adjustment of propeller P/D would increase the RPM. A two stage reduction, 4:1 at the pod and the rest at the engine would match the RPM, but probably cause bevel gear problems because the bevel gear would have to transmit the same power at reduced RPM.

It should be noted that for DTNSRDC propeller 3969-3 at $\sigma = .564$ (Reference 1) a pitch diameter change from 1.845 to 3.26 reduces the maximum efficiency from 70% to 65% and changes the corresponding thrust coefficient from .165 to .22 and the corresponding J values from 1.35 to 2.2. This data is presented to show the changes accompanying a pitch diameter change. Unfortunately propeller 3969-3 was not tested at a σ lower than .564 and therefore could not be used.

"ADDED DRAG" RATIOS OF STRUT POD UNITS						
	1000 TON Added Drag Ratio	No. of Prop.	2000 TON Added Drag Ratio	No. of Prop.	3000 TON Added Drag Ratio	No. of Prop.
100 KNOT DESIGN AT 100 KNOTS	1.36	3	1.35	4	1.31	6
80 KNOT DESIGN At 80 KNOTS	1.16	2	1.16	3	1.16	4
60 KNOT DESIGN At 60 KNOTS	1.10	2	1.08	3	1.08	3
Added Drag Ratio = $\frac{\text{Drag of Bare ACV} + \text{Strut} + \text{Pod}}{\text{Bare ACV Drag}}$						

Table 11 - Strut-Pod Added Drag Ratios

The added drag of the strut pod propulsion units is shown in Table 11. It is readily apparent that there is a high drag penalty associated with the 100 knot concepts. It is important to remember that each of the conceptual designs are for a particular L/B ratio and cushion pressure ratio. Optimization of these parameters greatly affects the powering feasibility of all the concepts examined. For example, a hump critical craft would benefit from an increase in L/B ratio and decrease in cushion pressure because the hump would be displaced to a higher speed and decreased in magnitude. By the same token, a concept which has a critical design speed capability would benefit from a L/B decrease and an increased cushion pressure since both of these changes would result in a decrease in drag at the design speed.

THE POWERING FEASIBILITY OF POINT DESIGNS

Qualitative Powering Feasibility Criteria

1. Design speed thrust power margin is represented by the ratio of thrust power required to thrust power available from 29.8 MW engine. If this ratio is the same for two craft with different design speeds, the lower speed craft involves less risk and is more feasible.
2. Hump considerations:
 - a. All conceptual designs meet the 20% hump thrust requirement
 - b. The propeller efficiency at hump varies proportionally with J (See Figure 14). Less risk is associated with the propeller thrust prediction at high J and η_0 than at low J and η_0 in the hump range of J 's between .3 and .4.
 - c. The hump thrust power available to hump thrust power required ratio is based on assumed engine performance characteristics and is therefore a less precise index than the design speed ratio of power available to power required.

3. The higher speed vehicles are inherently riskier. Propeller characteristics were extrapolated from a propeller test corresponding to 80 knot operation to the 100 knot speed. Strut pod cavitation inception predictions and hydrodynamic drag prediction are more likely to be in error at higher speeds.
4. Concepts with four or more propellers will experience more propeller interaction effects due to arrangement problems than the 2 or 3 propeller concepts and since propeller interaction is not accounted for, the powering prediction for the four or more propeller concepts is more optimistic than the powering predictions for the 2 or 3 propeller concepts.

The powering feasibility ranking of the selected concepts is greatly influenced by the discrete jumps in available thrust power. Depending on the number of engines used, some concepts become grossly overpowered by the addition of the last engine which provides sufficient power. Nevertheless, some statements can be made about which concepts are not likely to be feasible and which concepts look reasonable.

1. 1000 ton design
 - a. A one propeller one engine design is unfeasible due to insufficient hump power and an excessive 374 cm. propeller diameter required for hump thrust.
 - b. The 2 engine, 60 knot design is grossly overpowered, - a safe bet but a waste of engine power.
 - c. The 2 engine, 2 propeller, 80 knot design uses 73% of the available power at hump and leaves a large power margin for possible increase in drag due to inaccurate prediction.
 - d. The 3 propeller, 3 engine, 100 knot design uses 87% of the available power at design speed, and does not leave much room for 100 knot drag prediction error.
2. 2000 ton design
 - a. 2 engine, 2 propeller, 60 knot design uses 81% of the 34 MW available intermittent power. The 34 MW intermittent power is based on Figure 20, which is considered tenuous for powers above 29.8 MW. A 3 engine design is considered much safer.
 - c. 3 engine, 3 propeller, 80 knot design uses 88% of the available continuous power at 80 knots. There is not

much margin for design speed drag error. Due to the lower design speed this concept is less risky than the 100 knot, 1000 ton, 3 engine design which has about the same percentage of power used at design speed.

- d. 4 engine, 4 propeller, 100 knot design has insufficient power available at design speed. Even if the power is made available with uprated engines, gear problems would arise due to the large power requirement.

3. 3000 ton design

- a. A 2 engine design would have insufficient hump and design power.
- b. The 3 engine, 3 propeller, 60 knot designs require 66% of the available hump power and 85% of the design power of the 3000 ton designs, this concept requires the most hump power.
- c. 4 engine, 4 propeller, 80 knot designs require 96% of the available power at design, allowing for almost no error in design drag prediction.
- d. The 100 knot, 6 engine, 6 propeller design has insufficient design power.
- e. It appears that a 4 engine, 70 knot design would be reasonable to aim for.

2000 TON, 80 KNOT DESIGN ARRANGEMENTS AND CHARACTERISTICS

Time and funding limitations did not allow for the preparation of arrangement drawings nor for the graphic presentation of the calculated performance of all the concepts listed in Tables 8, 9, and 10. Instead these graphs and drawings were prepared only for one concept, chosen somewhat arbitrarily, the 2000 ton, 80 knot, 3 engine design.

The drag curve used for all the 2000 ton designs is presented in Figure 21. Note the 20% hump thrust margin and the increase in added drag as the design is changed to accommodate a 60, 80 and 100 knot top speed.

The propeller operating conditions at hump and design speed

for the 2000 ton, 80 knot design are shown in Figure 22. Note the shallow angle of intersection between the required thrust curve and the thrust curve of the propeller. This shallow angle indicates that the accuracy of the prediction is critical. The required thrust curve includes the 20% hump thrust margin. The design speed available and required thrust curve intersect at a shallow angle also, however an inaccuracy here will result only in a small change in top speed whereas an inaccuracy at hump could make the hump performance critical.

The 80 knot, 2000 ton ACV characteristics are presented in Table 12. Sketches of the craft were generated using these dimensions. Figure 23 shows a cross section arrangement that was judged undesirable due to the extreme outboard strut locations which would require shafting and right angle gears between the strut top and engine. Figure 24 shows the struts moved inboard and shortened to pivot about the point below the box structure. The pivot point and engines would be enclosed in a nacelle. A 3 dimensional view of this arrangement is shown in Figure 25 and the overall arrangement is shown in Figure 26.

CONCLUSIONS

It should be realized that the total feasibility of an ACV conceptual design cannot be established until an iterative design procedure involving the volume and weight requirements of thrust engines and the associated thrust systems, lift engines and associated lift systems, structure, fuel, payload and all other systems needed for the

2000 TON, 80 KNOT ACV Characteristics and Dimensions

Craft Dimensions	
Length of Cushion	= 60.5 M
Beam of Cushion	= 34.2 M
Day Light Gap	= .075 M
Cushion Height	= 7.3 M
Overall Height	= 14.5 M
Strut Pod Propeller Dimensions	
Pod Dia Max	= 94 cm
Pod Dia at Base	= 68 cm
Pod Length	= 404 cm
Strut Thickness at Base	= 31 cm
Strut Chord	= 174 cm
Propeller Diameter	= 226 cm
Other Features	
No. of Engines	= 3
No. of Strut Pod Propulsion units	= 3
Cushion Pressure Ratio, P_c/\sqrt{S}	= 350 N/M ³
Cushion Pressure	= 13,380 N/M ² = (279 PSF)
Static Head of Water Corresponding to 13,380 N/M ² Cushion Pressure	= 1.32 M

Table 12 - 2000 Ton 80 Knot ACV Characteristics and Dimensions

operation of the ACV is performed. In such a procedure applied to many concepts, a feasibility criteria has to be established based on conceptual mission requirements. For example, one might choose payload fraction for a transport mission. In this report, only powering feasibility is addressed and it is expected that the results will be used as input to an overall feasibility program.

Conclusions based on power requirements only: 1. The following three concepts appear to be the most feasible:

1. 1000 ton, 2 engines, 60 knot design
2. 1000 ton, 2 engines, 80 knot design
3. 2000 ton, 3 engines, 60 knot design

The 1000 ton, 60 knot design involves a waste of engine power at design speed. If such a design is contemplated, less powerful engines should be used.

2. A small error in drag and propeller thrust prediction will reduce the design speed of the following three concepts.

- 2000 ton, 80 knot, 3 engines
- 3000 ton, 80 knot, 4 engines
- 1000 ton, 100 knot, 3 engines

3. Of the 3000 ton designs, the 60 knot 3 engine design appears most feasible, however its hump performance is poorer than that of the 4 engine, 80 knot design. The 4 engine design will just barely reach 80 knots, but hump power is no problem. Perhaps a 70 knot 4 engine design will have a comfortable design speed power margin.

4. Of the 100 knot designs, only the 1000 ton, 3 engine design reaches design speed, however the design speed power margin is small. Hump power is not expected to be a problem.

5. A 40,000 HP engine, a 40,000 HP right angle dual mesh 1:1 bevel gearbox, and a 40,000 HP reduction gearbox with a reduction ratio in the 3.2:1 to 4:1 range appear to be within the near future state of art. Development work is needed on these items, but it is reasonable to count on using such hardware in near future ACV's.
6. A strut-pod Z drive arrangement with twin downshafts in the strut, 1:1 dual mesh spiral bevel gears and a reduction gear in the pod could be utilized to deliver 40,000 HP to the propeller.
7. For near future ACVs the pod reduction gear should be in the 3.2:1 to 4:1 range. A 2.285:1 reduction gearbox needs more development than the 3.2:1 or 4:1 gearbox. A 5.33:1 reduction gearbox results in excessive pod diameters.
8. The added drag ratio of the 100 knot designs is very high. It is approximately 1.35 for 100 knots, 1.16 for 80 and 1.08 for 60 knots. These ratios illustrate the high drag penalty associated with high speed.

RECOMMENDATIONS

1. Use an integrated approach to feasibility prediction. Optimize or match cushion pressure ratio, craft length-beam ratio, craft drag, propeller pitch diameter ratio to propulsor requirements and lift system requirement. Input simplified propeller stress limits, gear design constraints and possible strut side force structural limits to generate realistic Z drive designs.
2. When locked into a hardware oriented feasibility study, specify the hardware such as number of engines and generate craft displacements and speed envelopes of thrust produced per propulsion unit instead of arbitrarily specifying craft displacement and design speeds.
3. Develop a high speed controllable pitch supercavitating propeller series. Obtain open water characteristics by testing in a tunnel for a cavitation number $\sigma=7.0$ to $\sigma=0.09$ to cover both the hump and 100 knot design speed case. The DTNSRDC 3963 series is inadequate since the lowest σ tested was .564.

4. Improve strut pod hydrodynamic design procedures and drag predictions. Survey all available strut-pod performance data and performance prediction methods. If necessary, conduct strut-pod resistance experiments to verify or develop a reliable strut-pod prediction technique. Use the technique to optimize strut pod drag. Reference 5 suggests that a beneficial trade-off point exists between the friction, base and form drag of strut-pod units operating above 70 knots.

5. Demonstrate, on a model scale, the feasibility of operating a supercavitating propeller behind a base vented strut pod. Use a water tunnel or the hundred knot carriage at DTNSRDC demonstrate this feasibility. Measure strut-pod-propeller performance and obtain thrust deduction and wake fraction. Reliable thrust deduction and wake fraction values are needed.

REFERENCES

1. J. Toth and V. Zardus "Selection of a Hydrofoil Transmission and Propeller System," 1976 Grumman Aerospace Corp.
2. T. Csaky, "Advanced Transmission Study for a 2000 Ton SES," David W. Taylor Naval Ship R&D Center Report 27-674, 1974.
3. R. K. Muench, "Arctic Surface Effect Vehicle Program Parametric Data on a Mechanical Transmission Suitable for Large Surface Effect Vehicles," David W. Taylor Naval Ship R&D Center Report 27-650, 1973.
4. AGMA 226.01, "Geometry Factors for Determining the Strength of Spur, Helical, Herringbone and Bevel Gear Teeth.
5. E. Miller, et al, "A Parametric Analysis of Fast Hydrofoil Configurations," HYDRONAUTICS Technical Report, 7224-1, Nov 1972.
6. R. Hecker, et al, "Experimental Performance of TMB Supercavitating Propellers," Naval Ship R&D Center Report 1432, Jan 1964.
7. S.F. Hoerner, "Fluid Dynamic Drag," Midland Park, N.J., May 1951.
8. J. Strom-Tejsen and W.G. Day, "Study of Air Cushion Vehicle Propulsive System Part II, Engine Design and Performance," Naval Ship R&D Center, Ship Performance Department Report, SPD-378-H-07, Feb 1971.
9. "Experimental Performance of a Controllable Pitch Supercavitating Propeller," Naval Ship R&D Center Report 1636, Aug 1967.

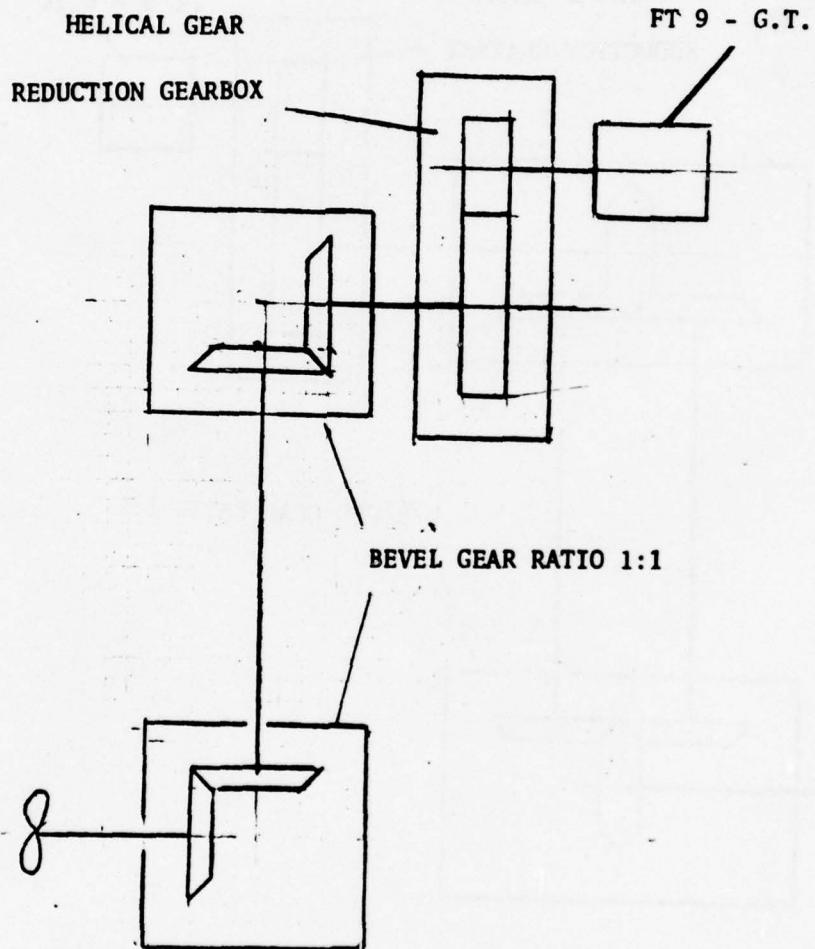


Figure 1 - Single Mesh Bevel Gear System - Reduction at Engine

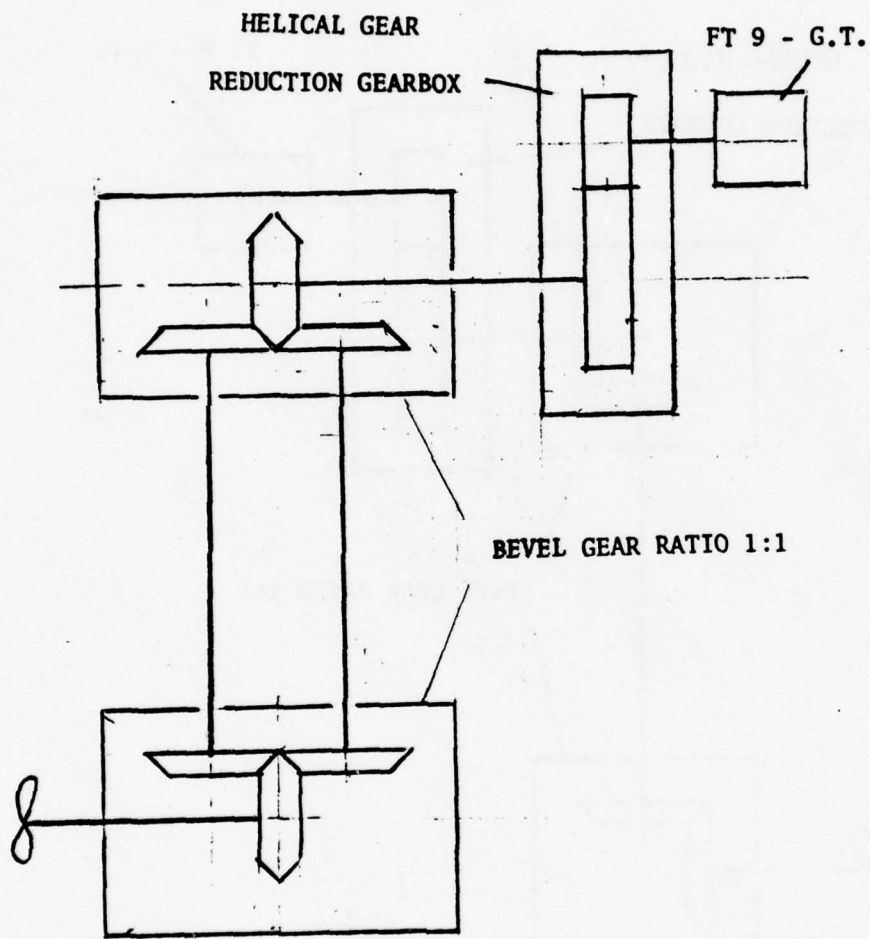


Figure 2 - Dual Mesh Bevel Gear System - Reduction at Engine

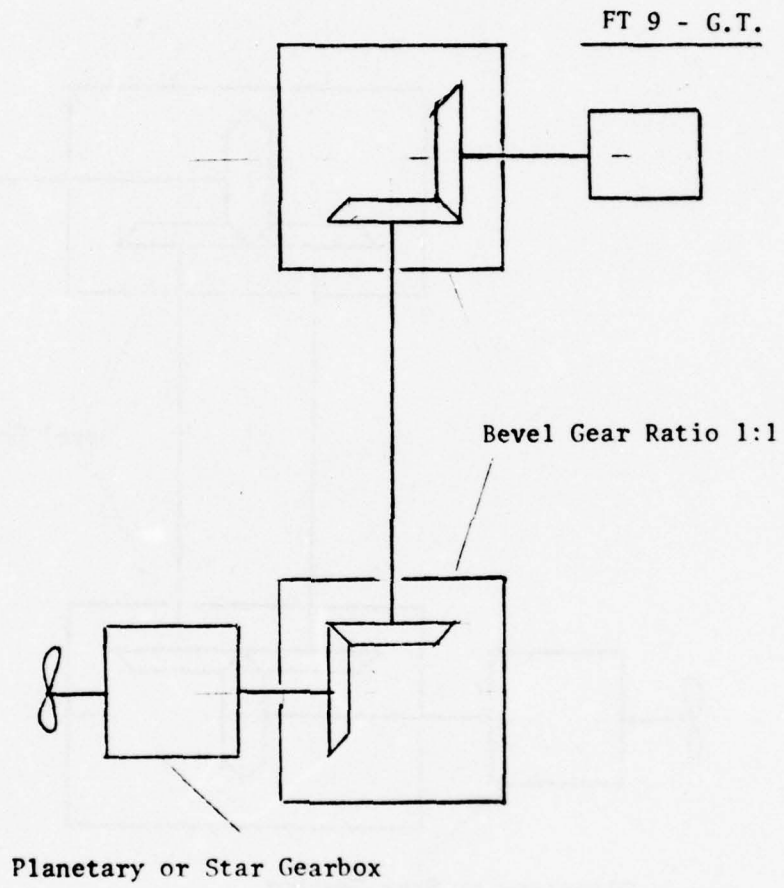


Figure 3 - Single Mesh Bevel Gear System - Reduction in Pod

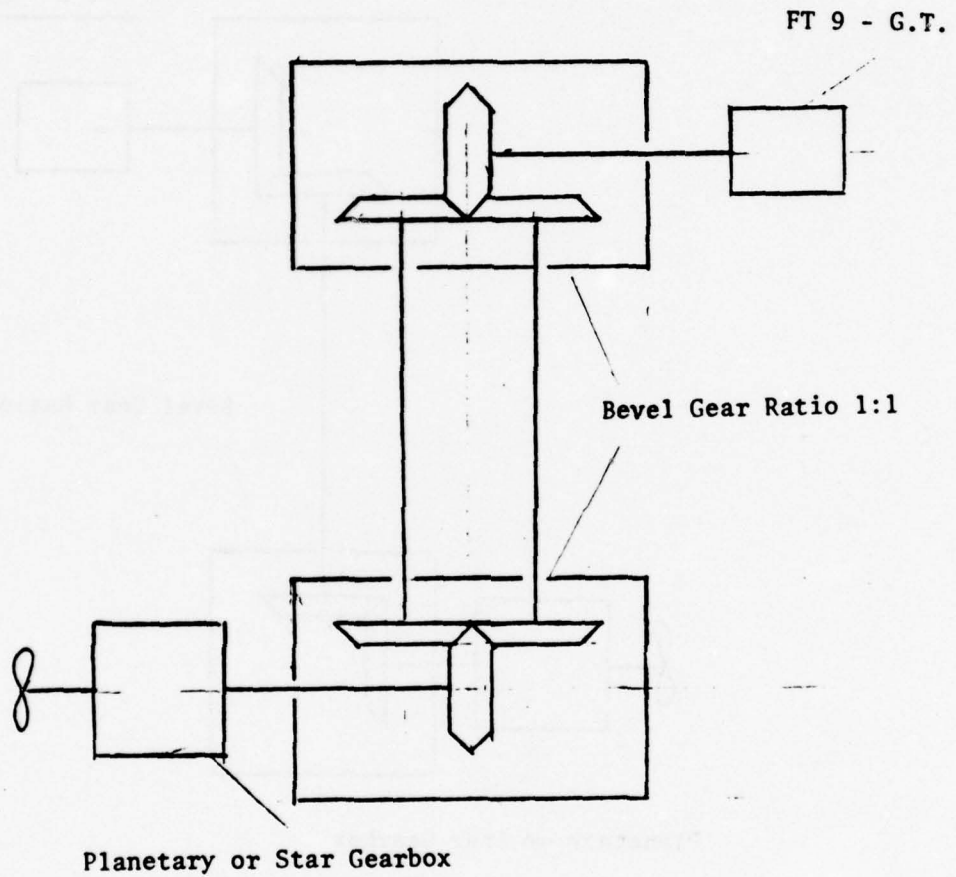


Figure 4 - Dual Mesh Bevel Gear System - Reduction in Pod

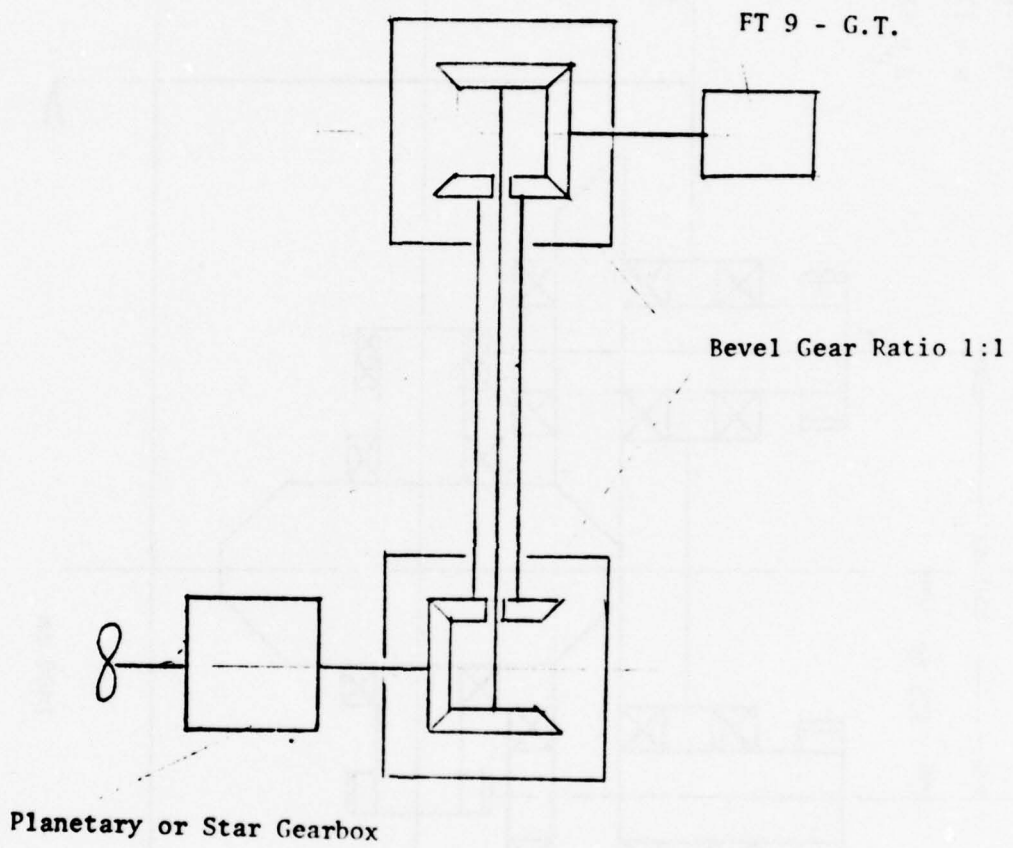


Figure 5 - Concentric Counterrotating Shafts

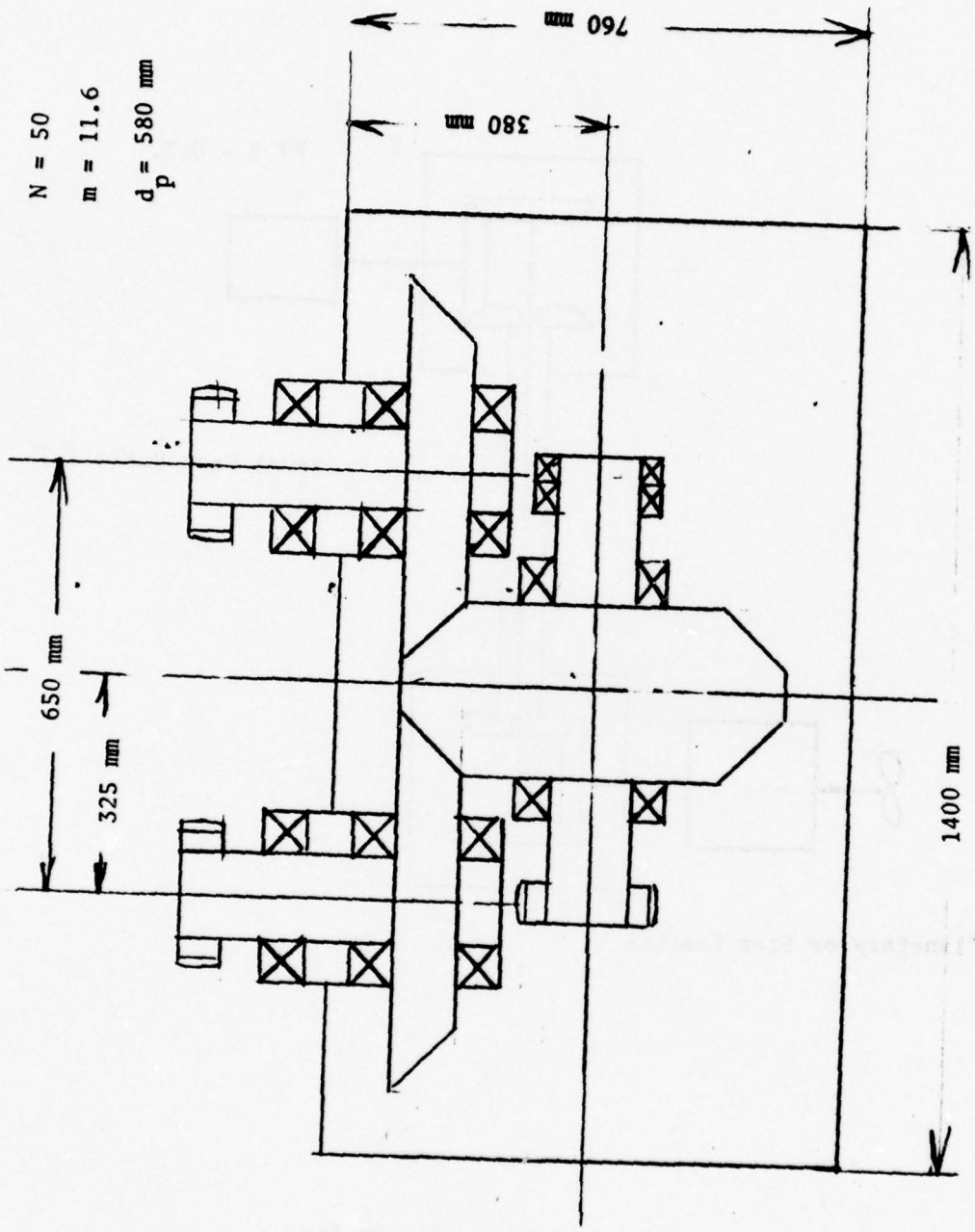


Figure 6 - Schematic of the Lower Bevel Gearbox

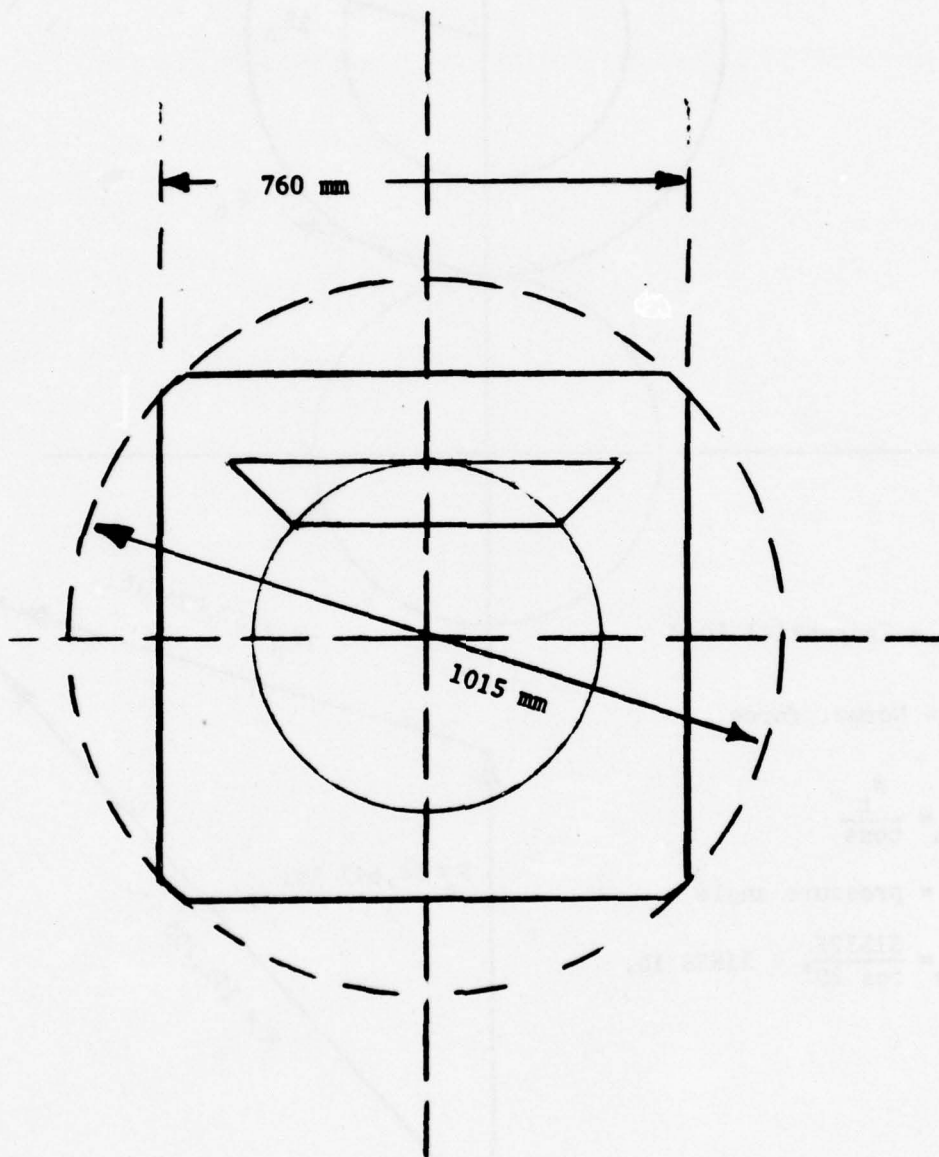
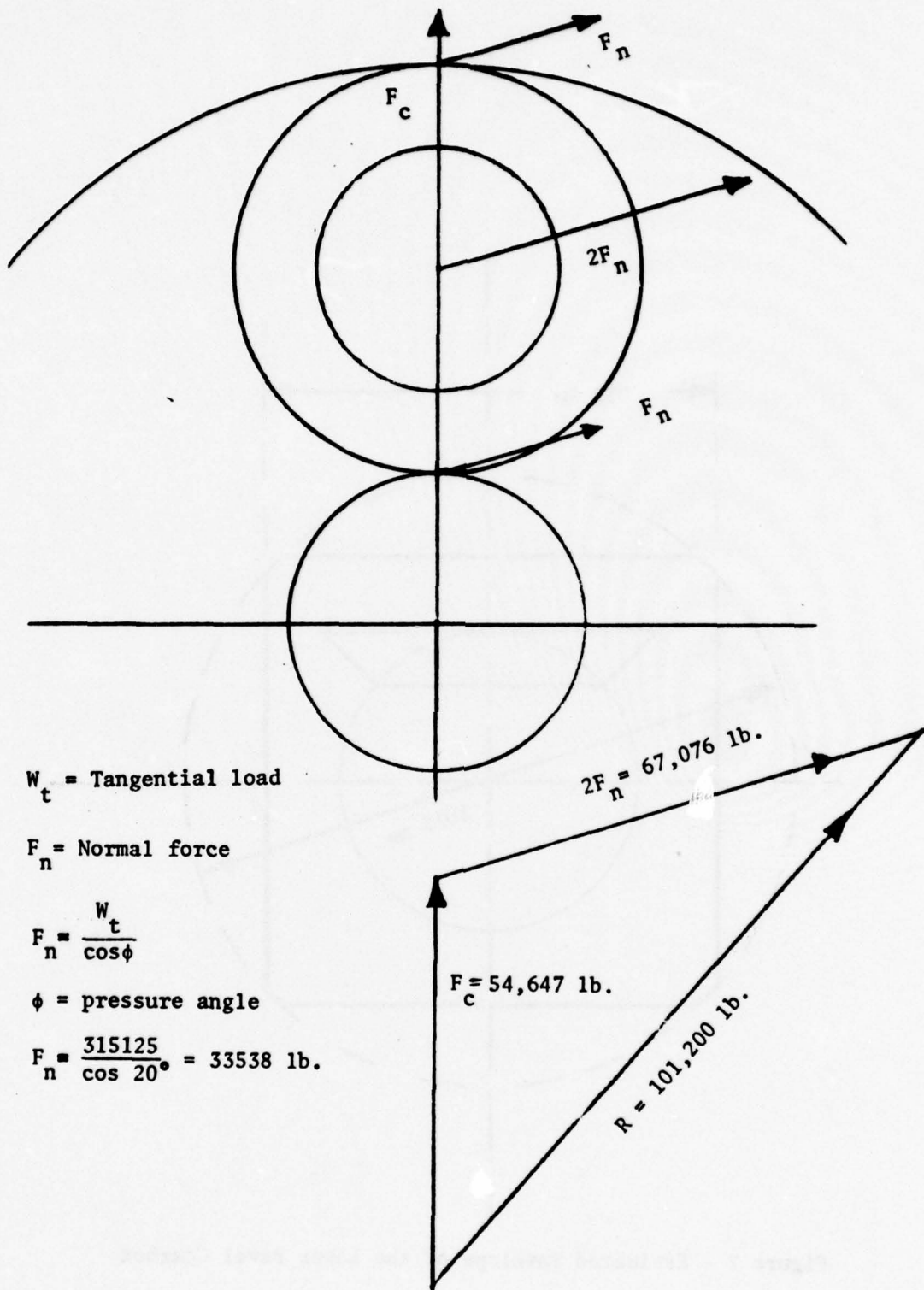


Figure 7 - Estimated Envelope of the Lower Bevel Gearbox



W_t = Tangential load

F_n = Normal force

$$F_n = \frac{W_t}{\cos \phi}$$

ϕ = pressure angle

$$F_n = \frac{315125}{\cos 20^\circ} = 33538 \text{ lb.}$$

Figure 8 - Loads on Planet Gear Shaft

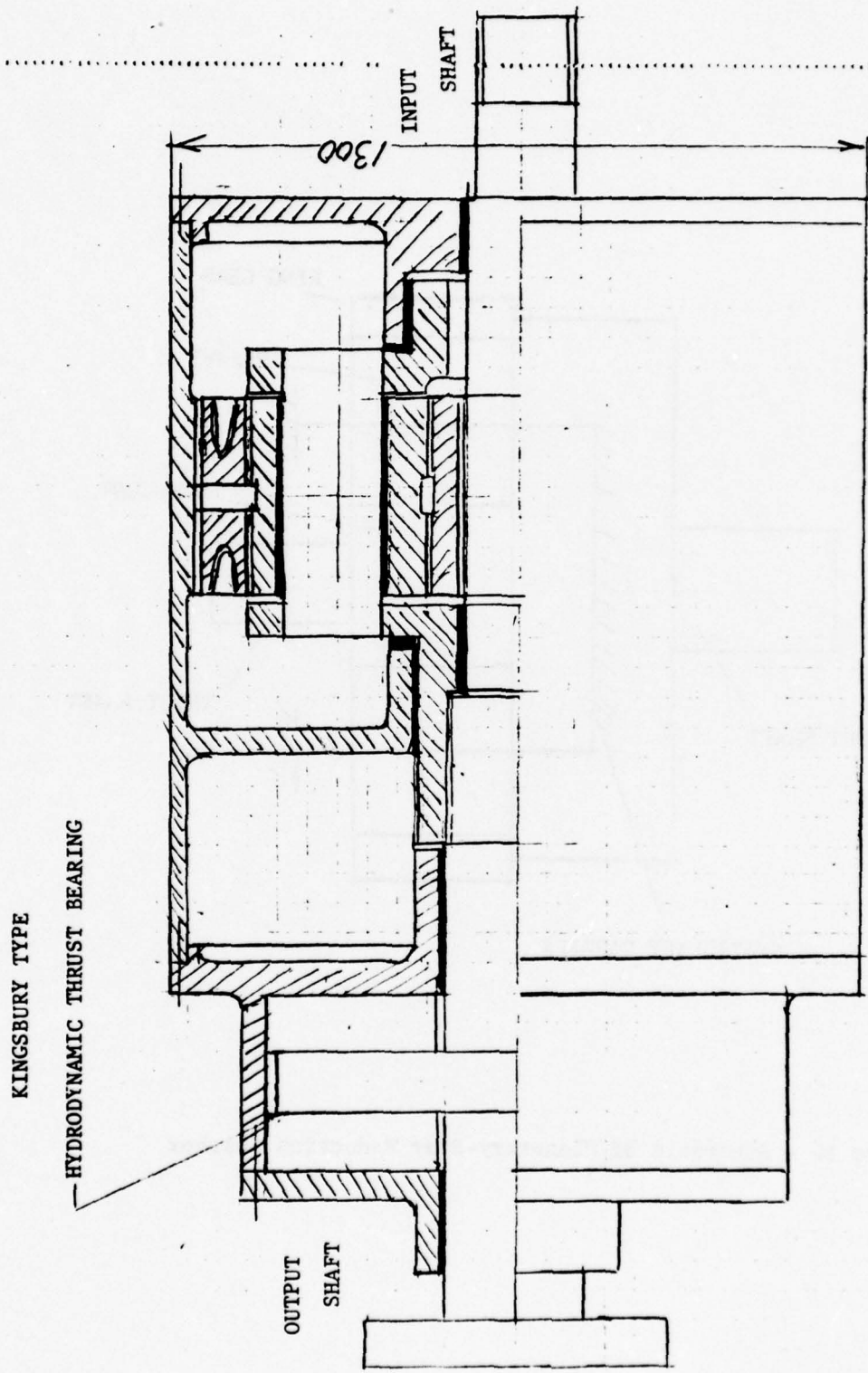


Figure 9 - Schematic of Planetary Gearbox with Stationary Ring Gear

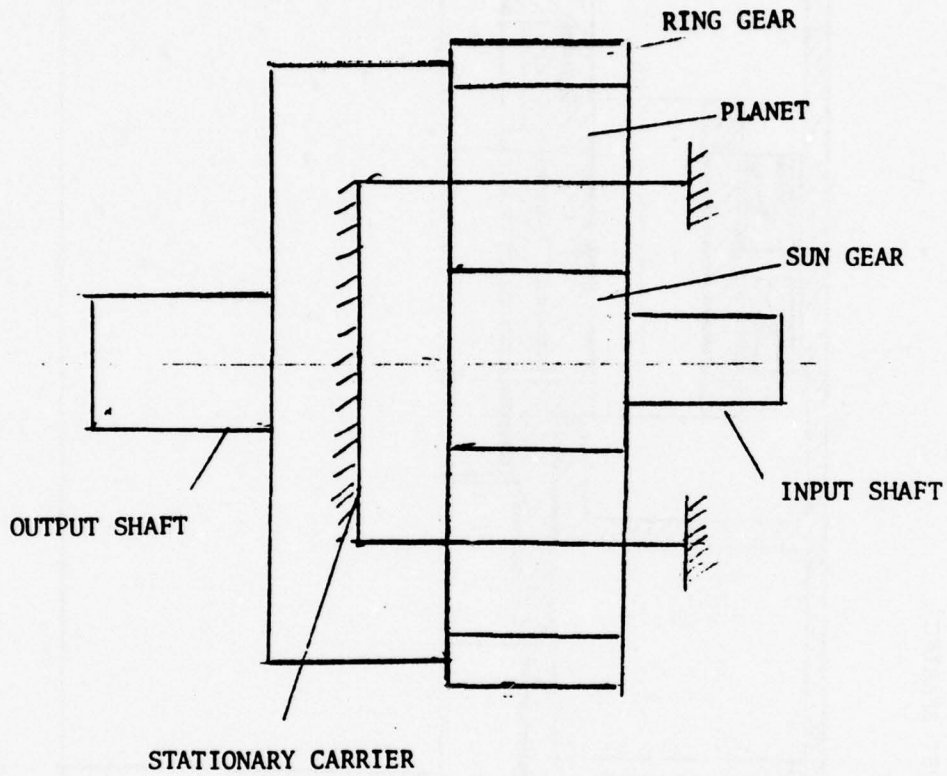


Figure 10 - Schematic of Planetary-Star Reduction Gearbox

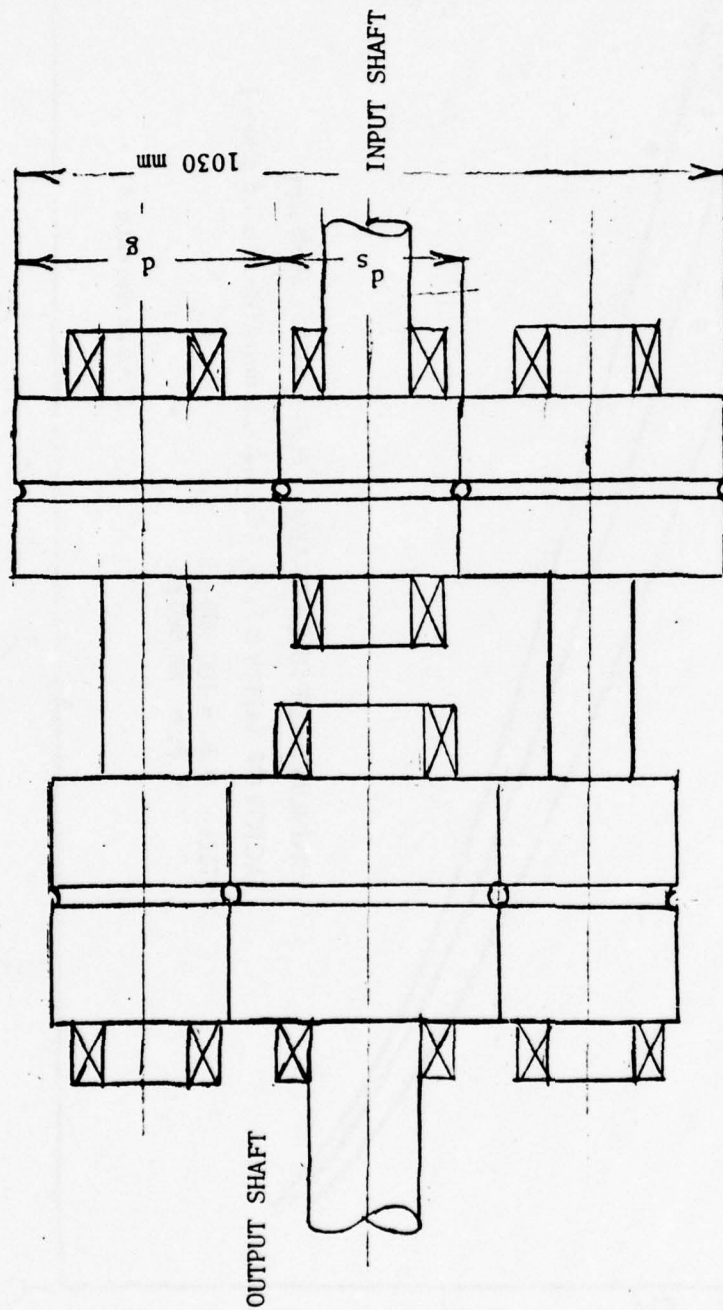


Figure 11 - Schematic of Multi Branched Concentric Double Reduction Gearbox

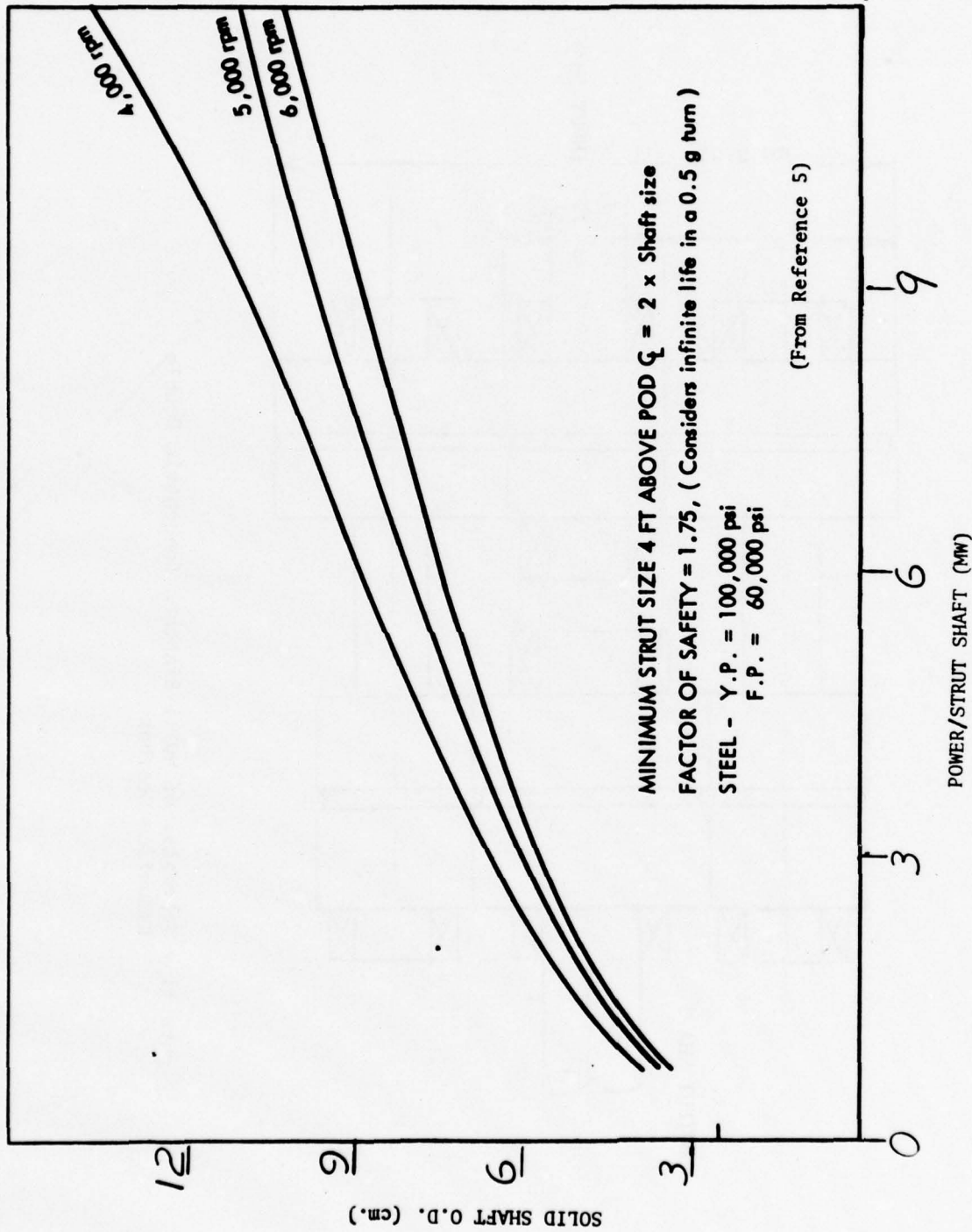


Figure 12 - Minimum Shaft Size for Required Horsepower per Shaft and Required RPM

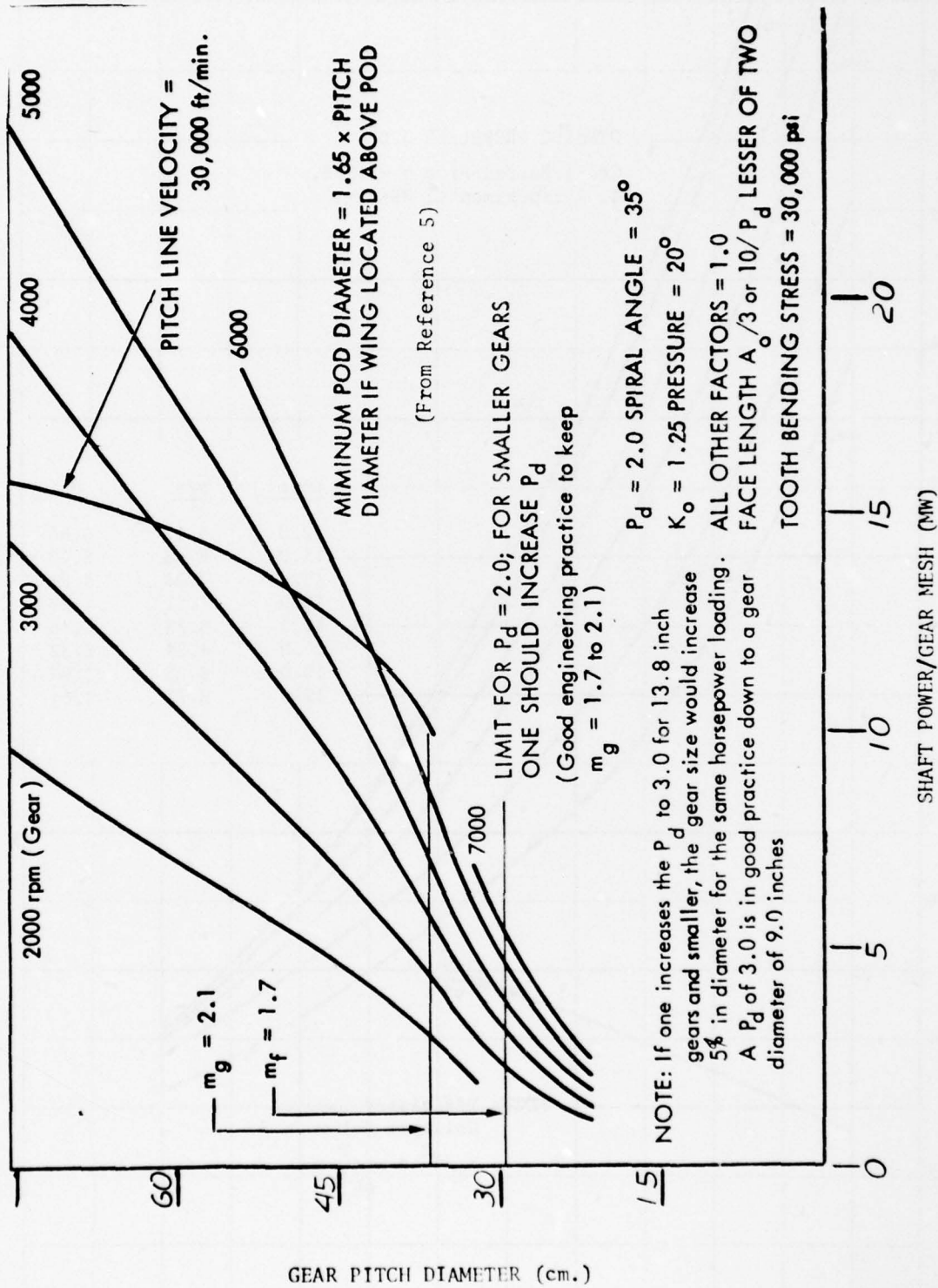


Figure 13 - Gear Pitch Diameters as a Function of Horsepower/Mesh RPM

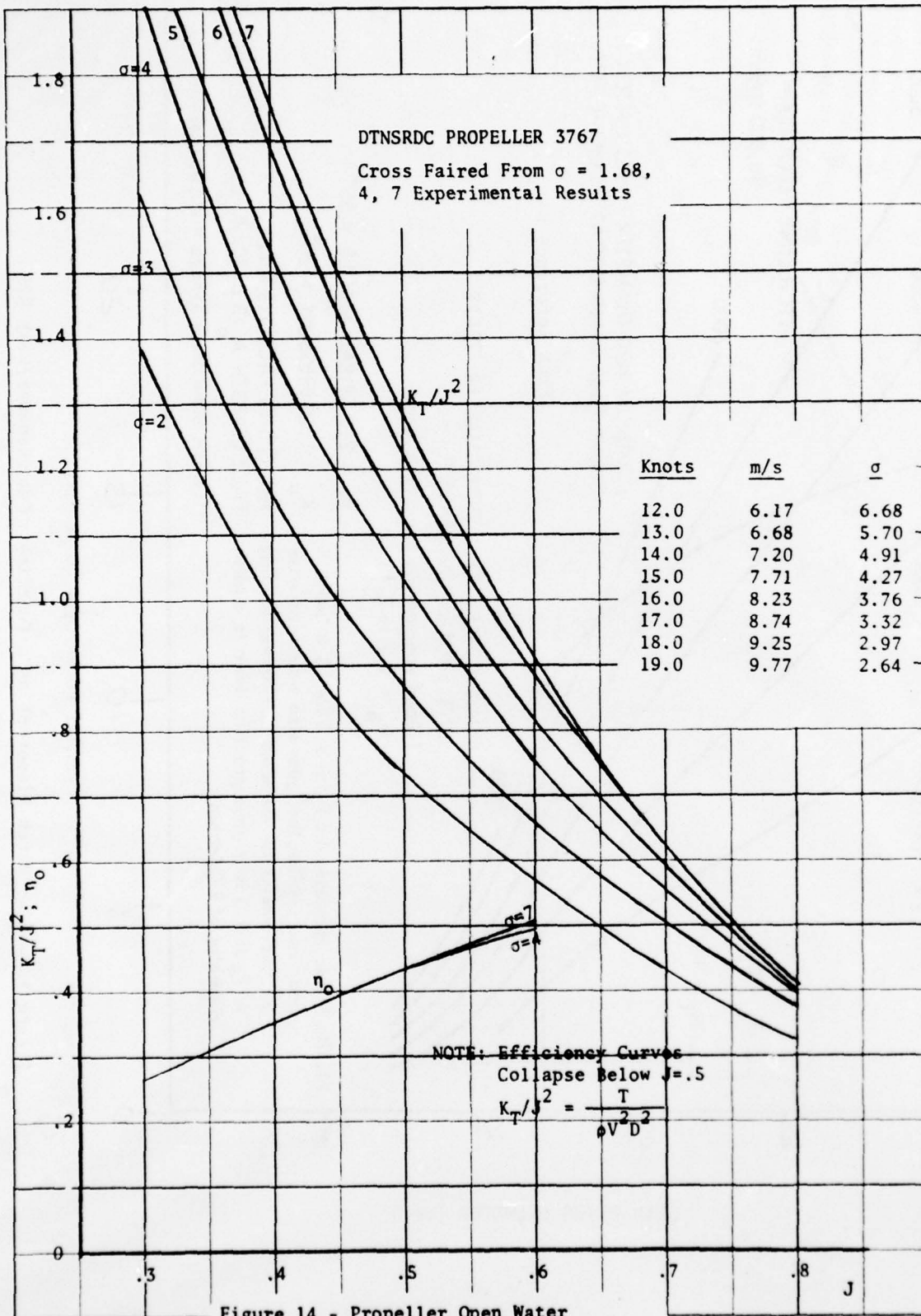


Figure 14 - Propeller Open Water
Performance Characteristics
at Hump

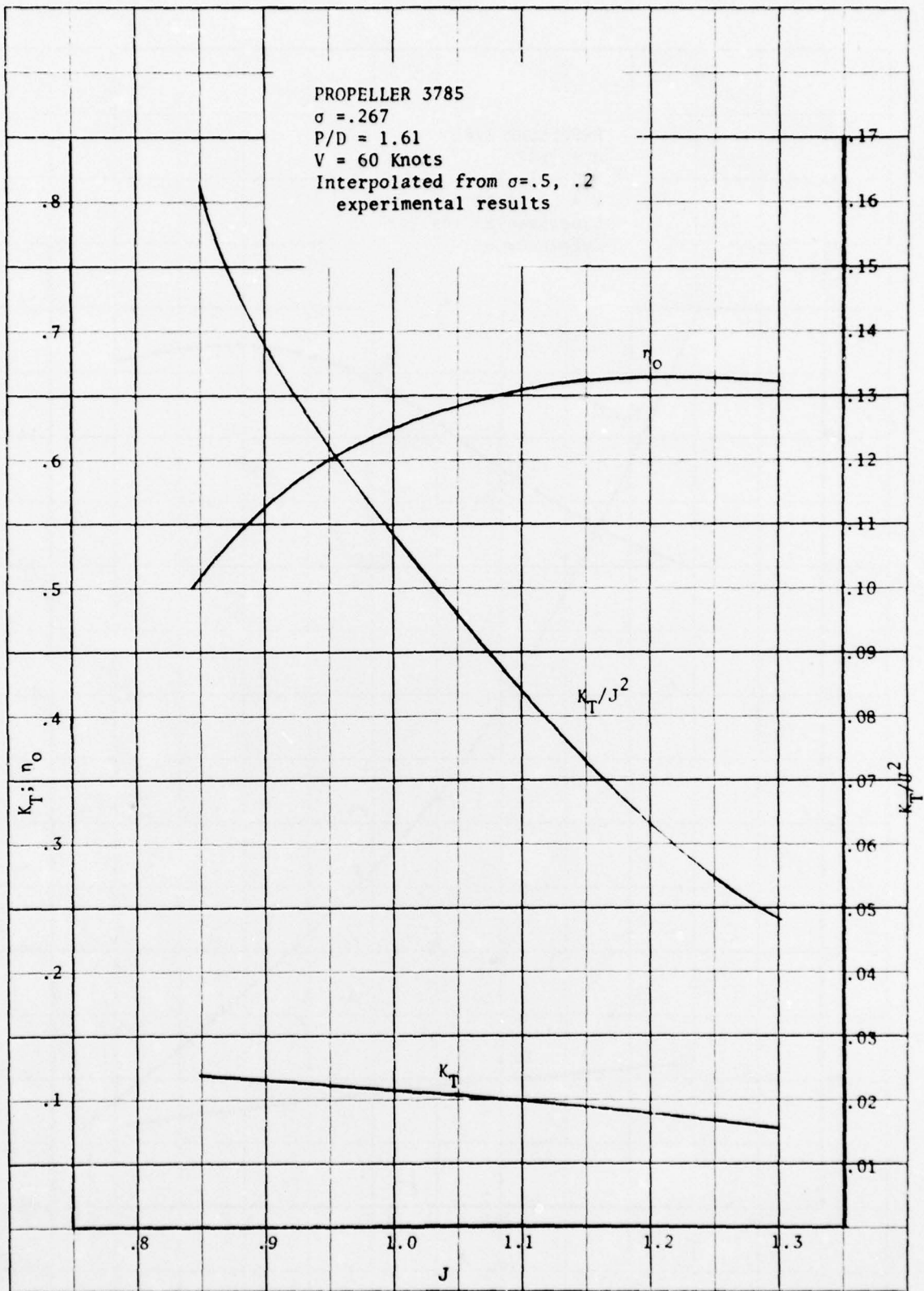


Figure 15 - Propeller Open Water Performance Characteristics at 60 Knots

PROPELLER 3785
 $\sigma = .147$
 $P/D = 1.61$
 $V = 80$ Knots
 Experimental results
 Reference 6

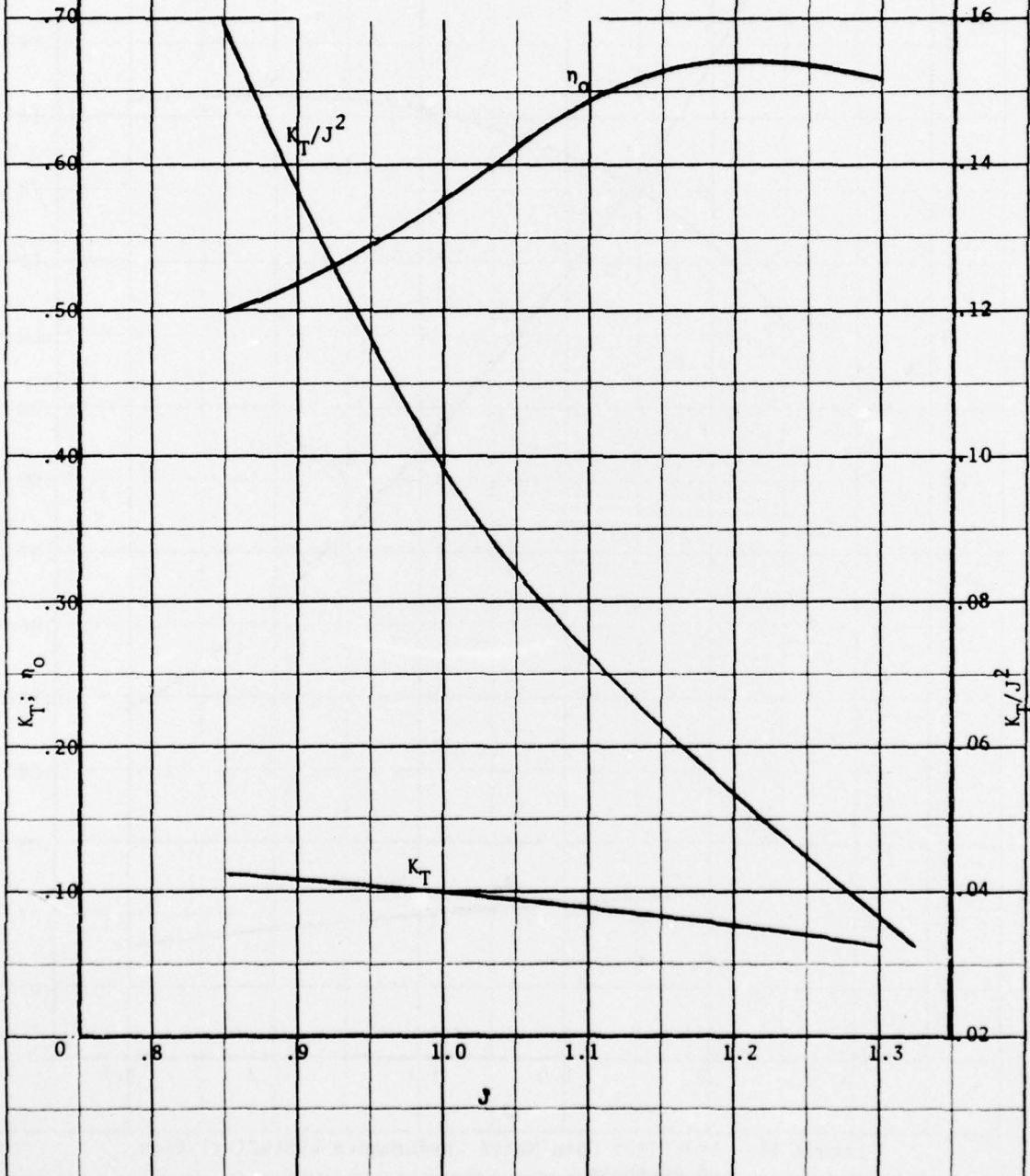


Figure 16 - Propeller Open Water Performance Characteristics at 80 Knots

PROPELLER 3785

$\sigma = 0.096$
 $v = 100$ Knots
 $P/D = 1.61$

EXTRAPOLATED PERFORMANCE
FROM $\sigma = 0.2, 0.147$
EXPERIMENTAL RESULTS

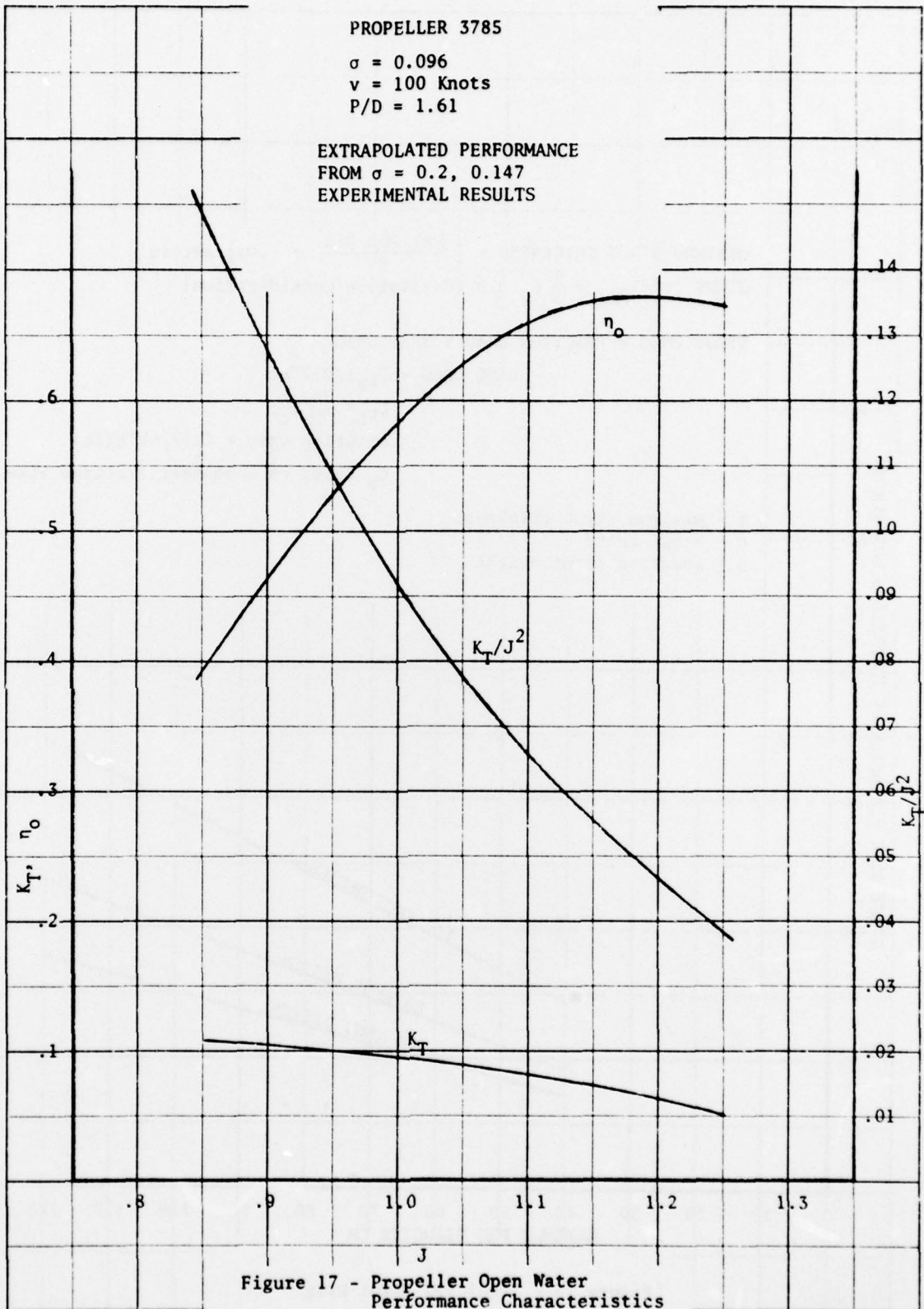
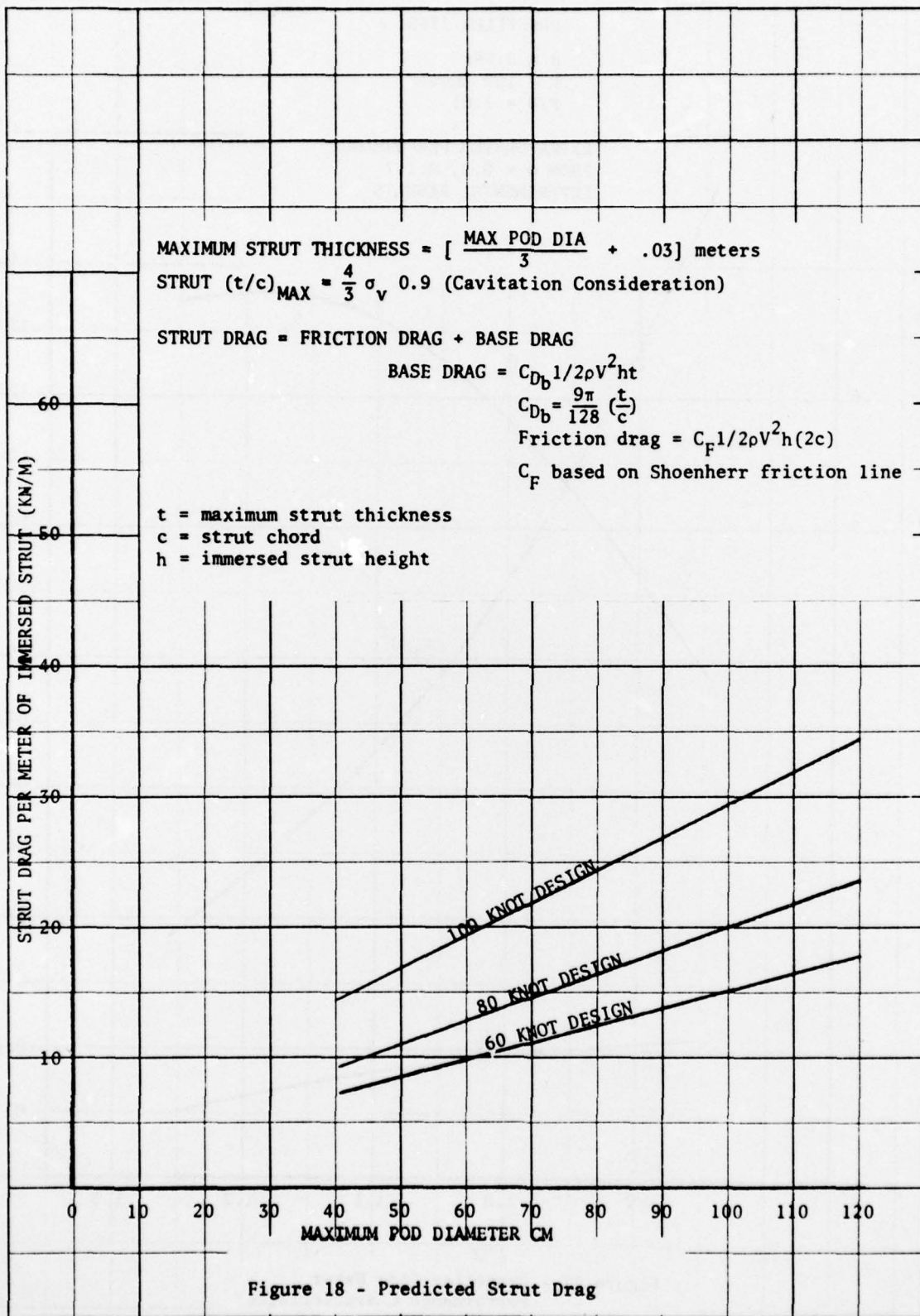


Figure 17 - Propeller Open Water Performance Characteristics at 100 Knots



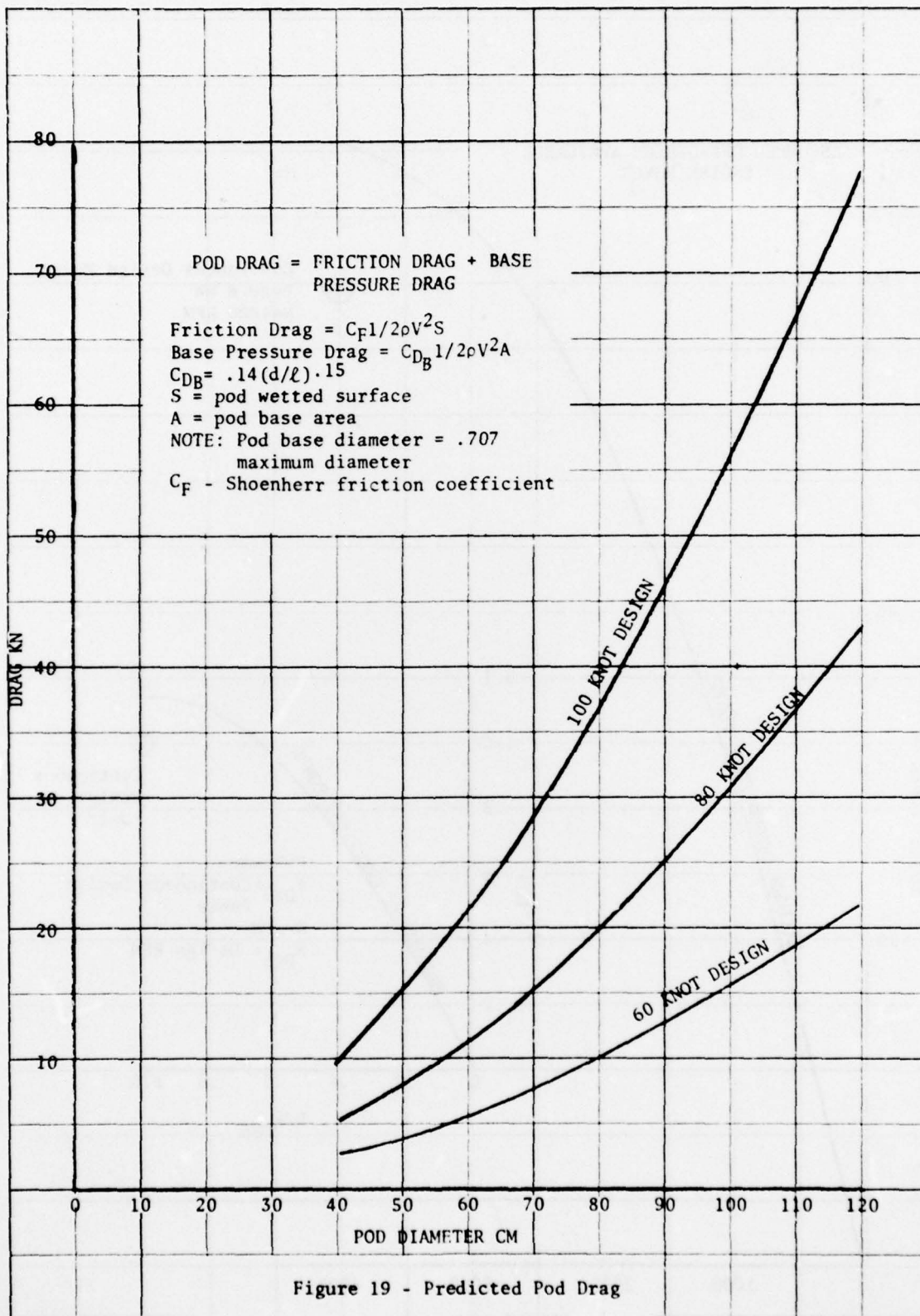


Figure 19 - Predicted Pod Drag

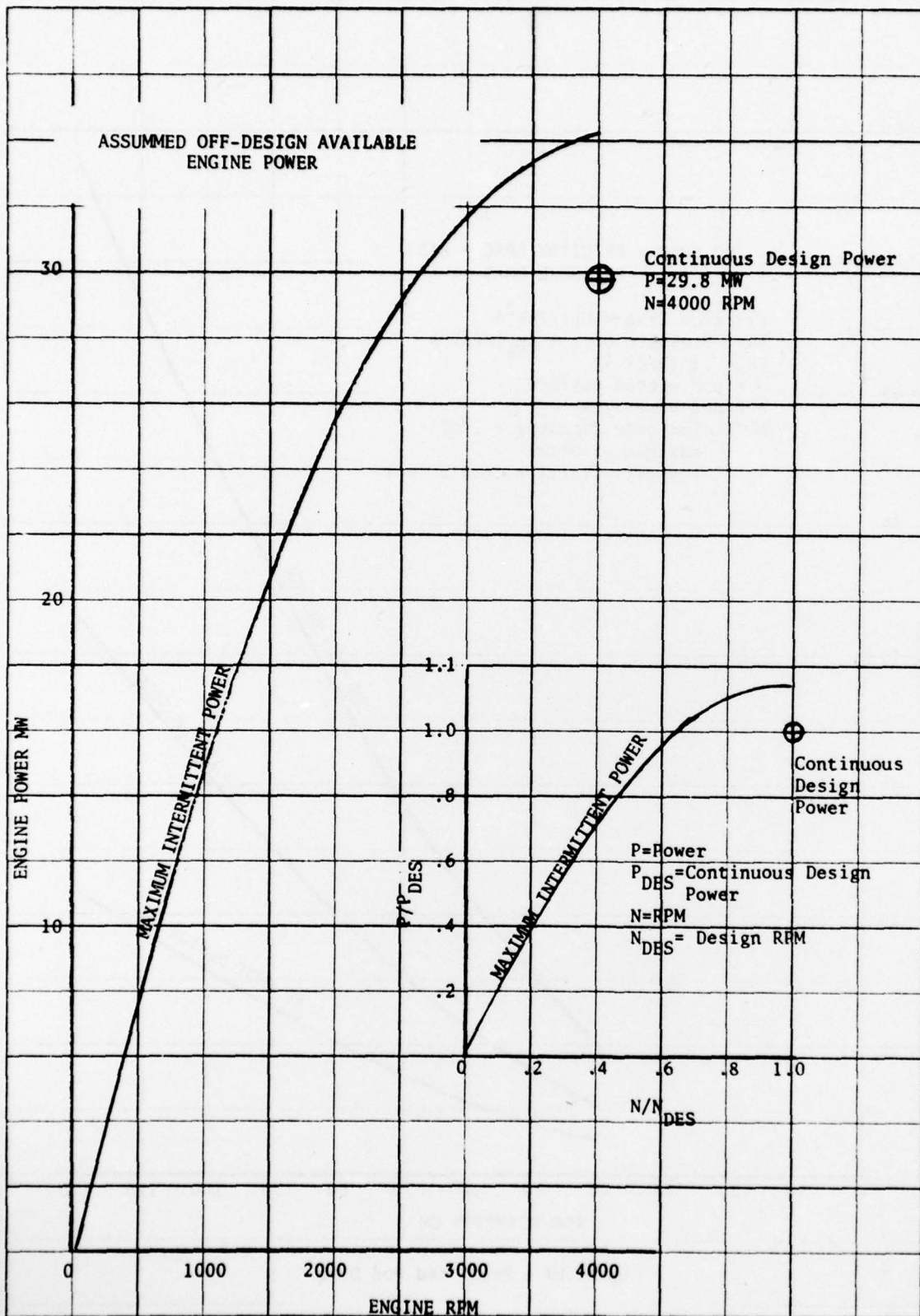


Figure 20 - Assumed Off-Design Available Engine Power

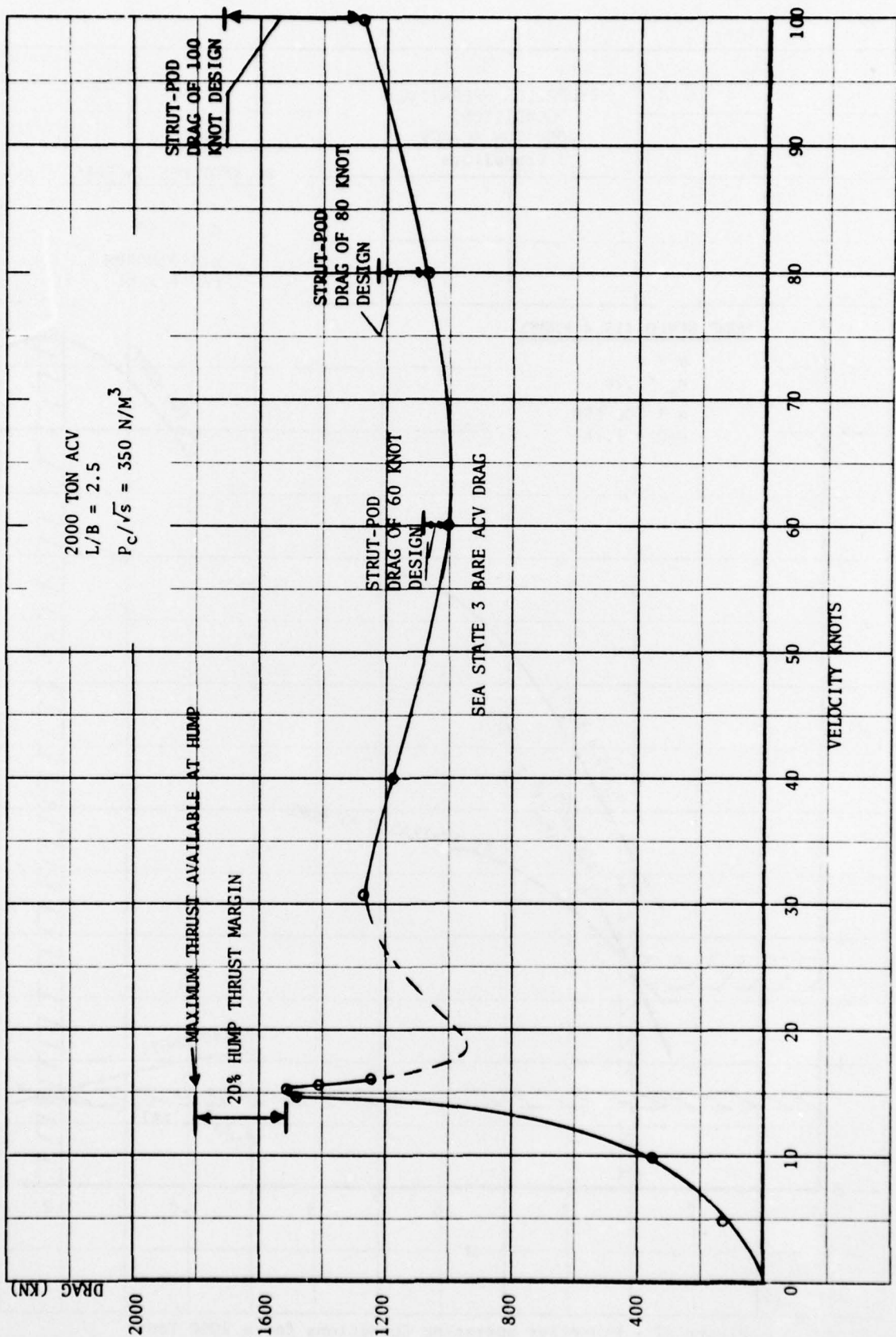


Figure 21 - Sample Drag Curve for 2000 Ton Designs

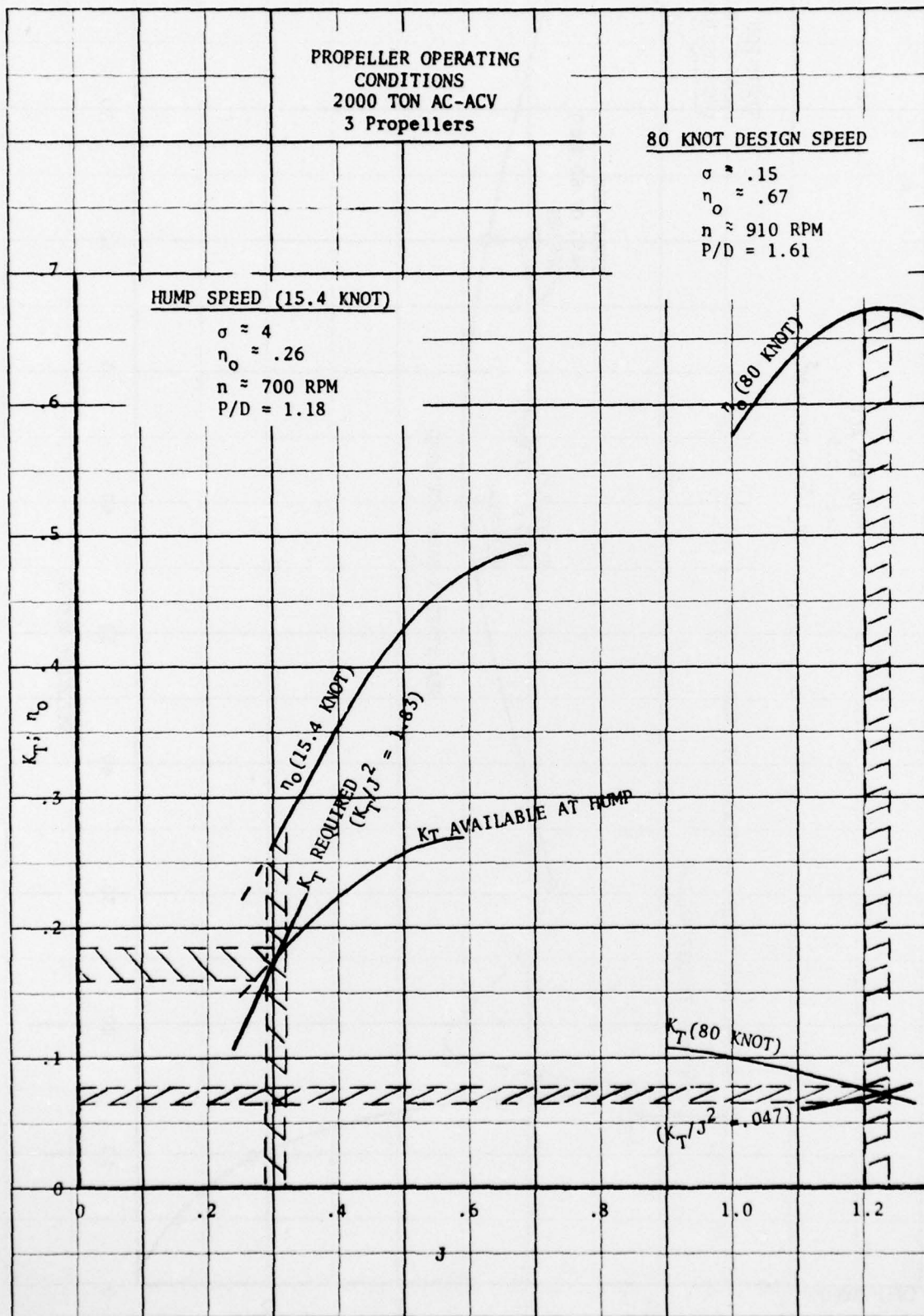


Figure 22 - Propeller Operating Conditions for a 2000 Ton,
80 Knot Design

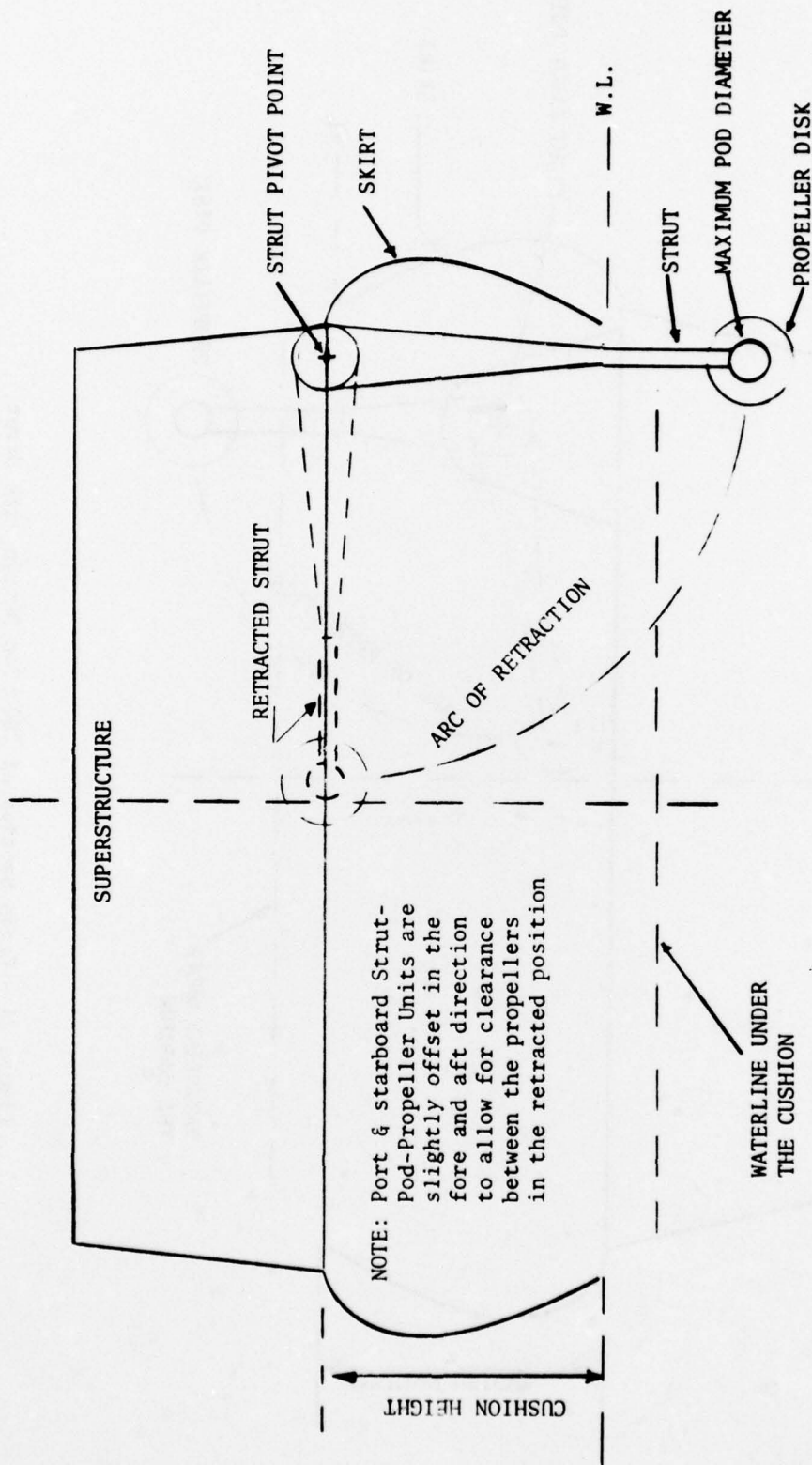


Figure 23 - Cross Section of 2000 Ton Design with Strut Pivoting at Box Structure Bottom

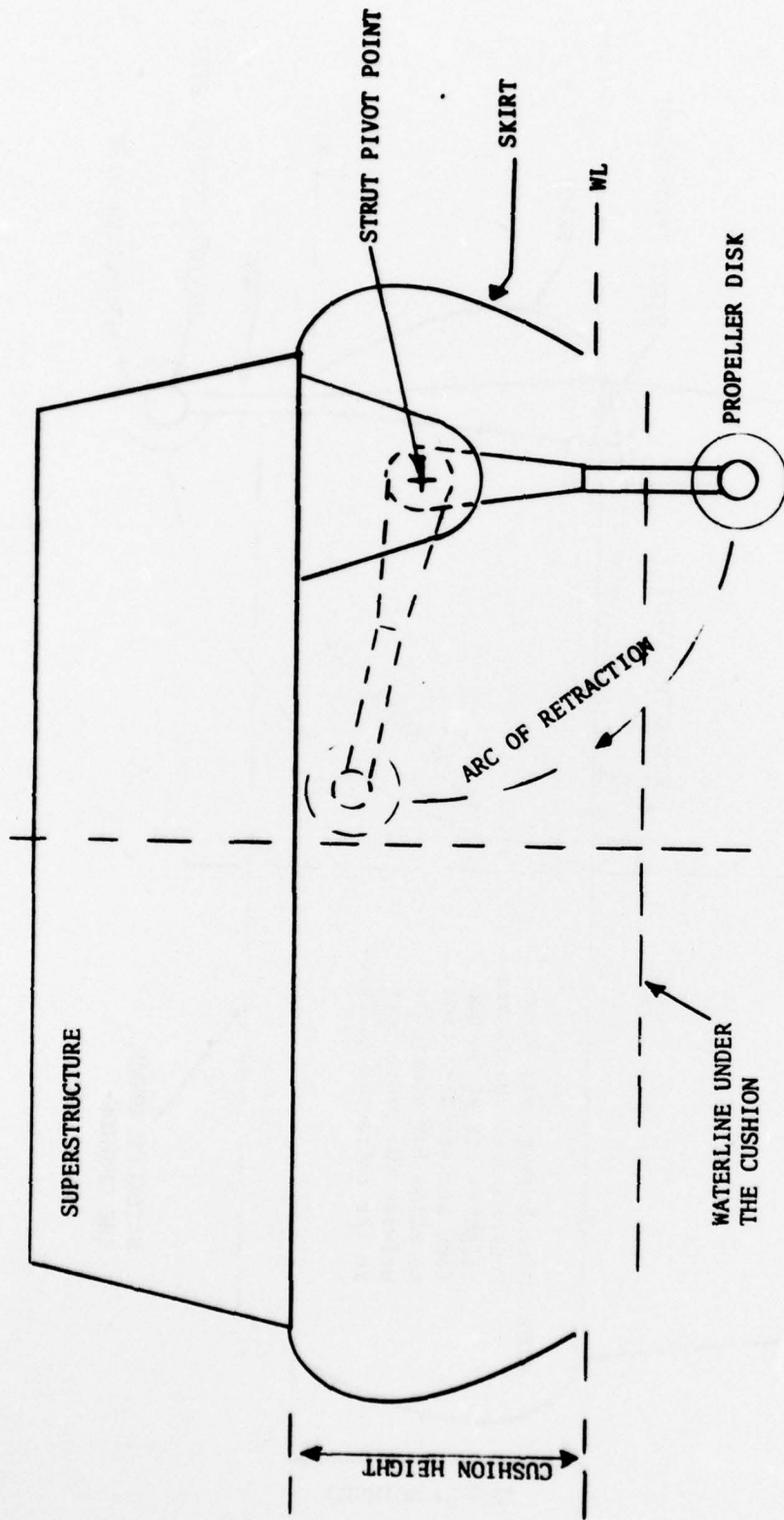


Figure 24 - Cross Section of 2000 Ton Design with Strut
Pivoting at Nacelle

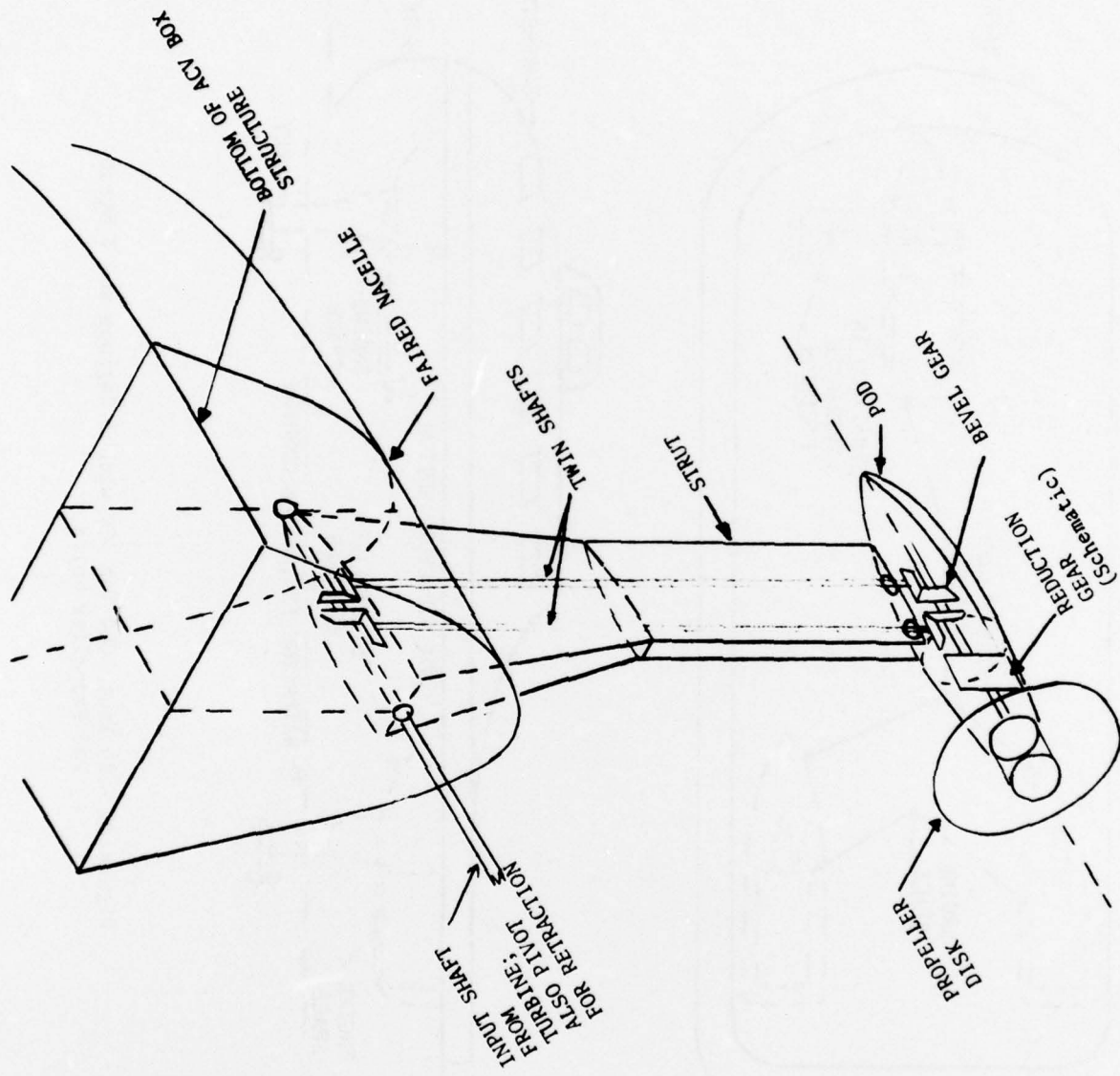


Figure 25 - 3-Dimensional View of Strut-Pod and Nacelle

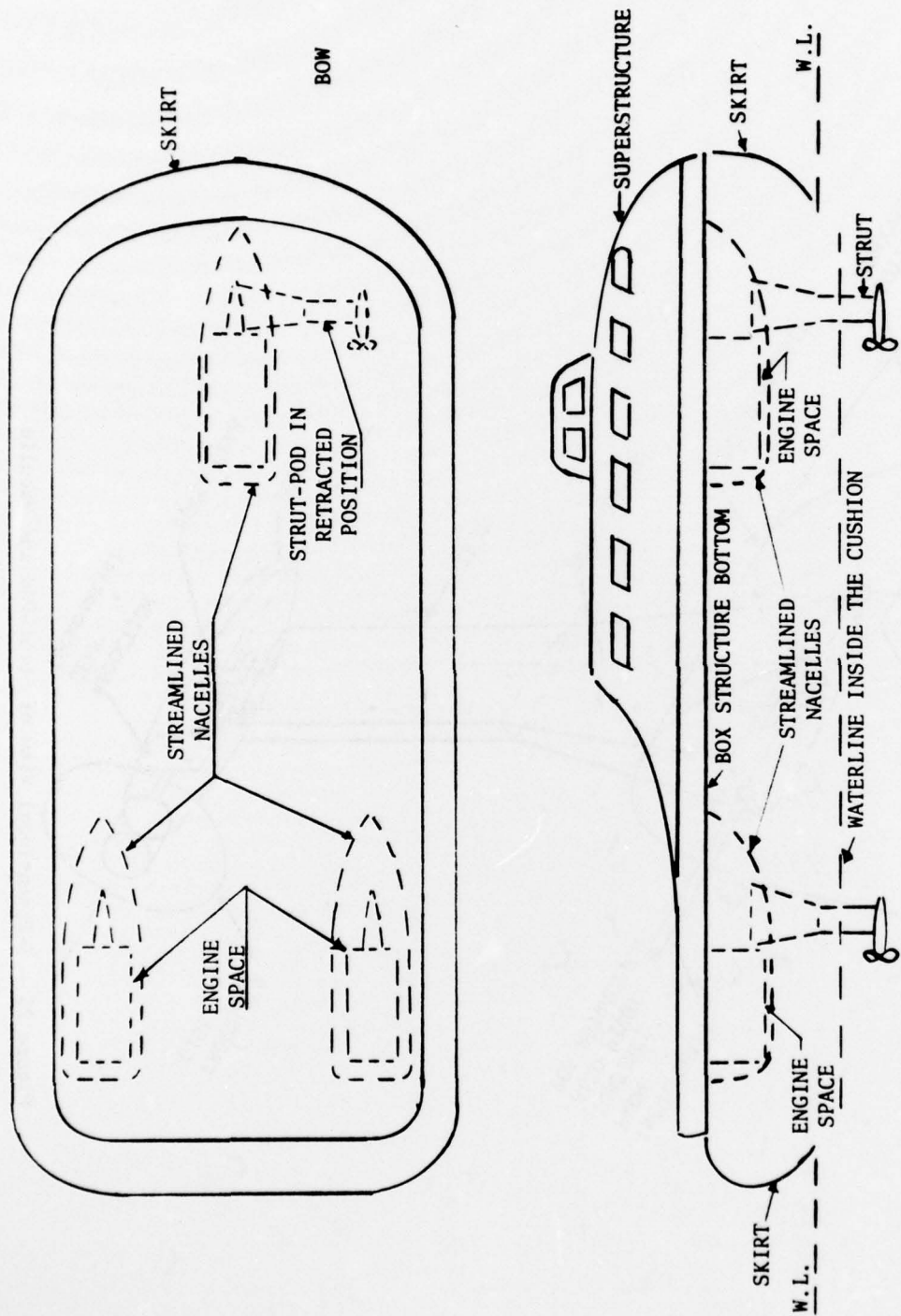


Figure 26 - 80 Knot 2000 Ton ACV with 3 Engines and 3 Strut Pod Propeller Units

DTNSRDC ISSUES THREE TYPES OF REPORTS

(1) DTNSRDC REPORTS, A FORMAL SERIES PUBLISHING INFORMATION OF PERMANENT TECHNICAL VALUE, DESIGNATED BY A SERIAL REPORT NUMBER.

(2) DEPARTMENTAL REPORTS, A SEMIFORMAL SERIES, RECORDING INFORMATION OF A PRELIMINARY OR TEMPORARY NATURE, OR OF LIMITED INTEREST OR SIGNIFICANCE, CARRYING A DEPARTMENTAL ALPHANUMERIC IDENTIFICATION.

(3) TECHNICAL MEMORANDA, AN INFORMAL SERIES, USUALLY INTERNAL WORKING PAPERS OR DIRECT REPORTS TO SPONSORS, NUMBERED AS TM SERIES REPORTS; NOT FOR GENERAL DISTRIBUTION.